A Regulated Adaptor Function of p40phox: Distinct p67phox Membrane Targeting by p40phox and by p47phox

Ueyama, Takehiko ; Tatsuno, Toshihiko ; Kawasaki, Takumi ; Tsujibe, Satoshi ; Shirai, Yasuhito ; Sumimoto, Hideki ; Leto, Thomas L. ;…

(Citation)
Molecular Biology of the Cell,18(2):441-454

(Issue Date)
2007-02

(Resource Type)
journal article

(Version)
Version of Record

(URL)
https://hdl.handle.net/20.500.14094/90000352

Molecular Biology of the Cell
Vol. 18, 441–454, February 2007

A Regulated Adaptor Function of p40^{phox}: Distinct p67^{phox} Membrane Targeting by p40^{phox} and by p47^{phox} [V]

Takehiko Ueyama,* Toshihiko Tatsuno,* Takumi Kawasaki,* Satoshi Tsujibe,* Yasuhito Shirai,* Hideki Sumimoto,† Thomas L. Leto,‡ and Naoaki Saito*

*Laboratory of Molecular Pharmacology, Biosignal Research Center, Kobe University, Kobe 657-8501, Japan; ‡Molecular Defenses Section, Laboratory of Host Defenses, National Institute of Allergy and Infectious Diseases, National Institutes of Health, Bethesda, MD 20892; and †Medical Institute of Bioregulation, Kyushu University, Fukuoka 812-8582, Japan

Submitted August 21, 2006; Revised November 13, 2006; Accepted November 14, 2006
Monitoring Editor: Ralph Isberg

In the phagocytic cell, NADPH oxidase (Nox2) system, cytoplasmic regulators (p47^{phox}, p67^{phox}, p40^{phox}, and Rac) translocate and associate with the membrane-spanning flavocytochrome b_{558}, leading to activation of superoxide production. We examined membrane targeting of phox proteins and explored conformational changes in p40^{phox} that regulate its translocation to membranes upon stimulation. GFP-p40^{phox} translocates to early endosomes, whereas GFP-p47^{phox} translocates to the plasma membrane in response to arachidonic acid. In contrast, GFP-p67^{phox} does not translocate to membranes when expressed alone, but it is dependent on p40^{phox} and p47^{phox} for its translocation to early endosomes or the plasma membrane, respectively. Translocation of GFP-p40^{phox} or GFP-p47^{phox} to their respective membrane-targeting sites is abolished by mutations in their phox (PX) domains that disrupt their interactions with their cognate phospholipid ligands. Furthermore, GFP-p67^{phox} translocation to either membrane is abolished by mutations that disrupt its interaction with p40^{phox} or p47^{phox}. Finally, we detected a head-to-tail (PX–Phox and Bem1 [PB1] domain) intramolecular interaction within p40^{phox} in its resting state by deletion mutagenesis, cell localization, and binding experiments, suggesting that its PX domain is inaccessible to interact with phosphatidylinositol 3-phosphate without cell stimulation. Thus, both p40^{phox} and p47^{phox} function as diverse p67^{phox} "carrier proteins" regulated by the unmasking of membrane-targeting domains in distinct mechanisms.

INTRODUCTION

In phagocytic cells, reactive oxygen species (ROS) are produced by NADPH oxidase (Nox2 system). The enzyme is a multiprotein complex assembled from a membrane-spanning flavocytochrome b_{558} (composed of gp91^{phox} [Nox2] and p22^{phox}) and four cytoplasmic components (p47^{phox}, p67^{phox}, p40^{phox}, and Rac) (Leto, 1999; Nauseef, 2004; Quinn and Gauss, 2004). In unstimulated phagocytes, the oxidase is dissociated and inactive: the flavocytochrome b_{558} is stored on the membranes of intracellular granules (Jesaitis *et al*., 1990), Rac is maintained in a GDP-bound cytoplasmic complex dimerized with Rho-guanine nucleotide dissociation inhibitor (GDI) (Bokoch *et al*., 1994), and the other phox proteins associate in a separate ternary cytoplasmic complex (p47^{phox}-p67^{phox}-p40^{phox}) in a dephosphorylated state (Bolscher *et al*., 1989; Rotrosen and Leto, 1990; Kuribayashi *et al*., 2002; Lapouge *et al*., 2002). During phagocyte activation, intracellular granules containing flavocytochrome b_{558} fuse with phagosomes; p47^{phox} is phosphorylated, thereby inducing conformational changes in p47^{phox} that promote the interaction of the cytoplasmic complex with the flavocytochrome b_{558}; and Rac dissociates from Rho-GDI and translocates independently to the membrane after exchange of GDP for GTP (Heyworth *et al*., 1994; Zhao *et al*., 2003), resulting in generation of superoxide anion by the transfer of electrons from cytoplasmic NADPH to molecular oxygen.

Chronic granulomatous disease (CGD), characterized by defective microbial killing by phagocytic cells, is caused by defects or deficiencies in any one of four oxidase components: Nox2, p22^{phox}, p47^{phox}, or p67^{phox} (Leto, 1999). An essential role for Rac1 or Rac2 in Nox2 activation was also identified in cell-free reconstitution studies (Abo *et al*., 1991; Knaus *et al*., 1991). This role was later confirmed in an oxidase-deficient patient who expressed mutant Rac2 (Ambruso *et al*., 2000; Williams *et al*., 2000) and in mice rendered genetically deficient in Rac2 (Roberts *et al*., 1999; Gu *et al*., 2003). Rac and p67^{phox} together have a direct roles in regulating electron flow through the flavocytochrome b_{558} through GTP-dependent interactions; hence, p67^{phox} is called an "activator" component (Bokoch and Diebold, 2002). Alternatively, p47^{phox} is called an "adaptor" or "organizer" component because it binds to membrane lipids [phosphatidylinositol-(3,4)-bisphosphate [PI(3,4)P_2] and phosphatidic acid (PA)] through its phox (PX) domain (Kanai *et al*., 2001; Karathanassis *et al*., 2002), is tethered to the flavocytochrome b_{558} through direct interactions between p22^{phox} and its Src homology (SH) 3 domain, and is linked to other cytoplasmic phox proteins to this complex (Leto *et al*., 1994; Sumimoto *et*

This article was published online ahead of print in *MBC in Press* (http://www.molbiolcell.org/cgi/doi/10.1091/mbc.E06–08–0731) on November 22, 2006.

[V] The online version of this article contains supplemental material at *MBC Online* (http://www.molbiolcell.org).

Address correspondence to: Naoaki Saito (naosaito@kobe-u.ac.jp).

Abbreviations used: AA, arachidonic acid; FcγR, Fcγ receptor; PA, phosphatidic acid; ROS, reactive oxygen species.

al., 1994). CGD patients who lack p47^{phox} show impaired translocation of p67^{phox} to the particulate or membrane fraction, whereas CGD patients who lack p67^{phox} show normal translocation of p47^{phox} to the particulate fraction, indicating the adaptor function of p47^{phox} in recruitment of p67^{phox} to the membrane (Heyworth *et al*., 1991; Dusi *et al*., 1996; Allen *et al*., 1999). However, Nox2 activity can be reconstituted in vitro in the absence of p47^{phox}, when p67^{phox} and Rac1 are provided in excess (Freeman and Lambeth, 1996; Koshkin *et al*., 1996) or when p67^{phox} is adapted with the membrane-binding sequences from Rac1, although GTP-bound Rac is still required for oxidase activation (Gorzalczany *et al*., 2000; Alloul *et al*., 2001), indicating p67^{phox} and Rac1 are minimum essential cytoplasmic components in the Nox2 system. p40^{phox} also has a PX domain that specifically binds to phosphatidylinositol 3-phosphate [PI(3)P] (Bravo *et al*., 2001; Kanai *et al*., 2001), a phospholipid enriched in the early endosome (Gillooly *et al*., 2000) and produced in the phagosomal membrane during phagocytosis (Ellson *et al*., 2001a; Gillooly *et al*., 2001). Thus, p40^{phox} is also thought to serve as an adaptor component that recruits p67^{phox} to phagosomal membranes (Kuribayashi *et al*., 2002). There are, however, no reports of p40^{phox} defects or deficiencies resulting in CGD. There is some controversy on the precise function of p40^{phox}, because both Nox2-inhibitory (Sathyamoorthy *et al*., 1997; Vergnaud *et al*., 2000; Lopes *et al*., 2004) and Nox2-supporting effects of p40^{phox} (Tsunawaki *et al*., 1996; Cross, 2000; Ellson *et al*., 2001b; Kuribayashi *et al*., 2002; He *et al*., 2004) have been reported. However, recent studies in p40^{phox}-deficient mice or in FcγIIA receptor-reconstituted cells indicate p40^{phox} is an essential component of the Nox2 system (Ellson *et al*., 2006; Suh *et al*., 2006).

Arachidonic acid (AA) has been used frequently as a activator of Nox2 in cell-free assay systems (Bromberg and Pick, 1984; Curnutte, 1985). Although relatively high concentrations of AA (50–200 μM) are required for activation of Nox2 both in vitro and in vivo, functional roles for cytosolic phospholipase A_2 (cPLA_2), which produces AA, in Nox2 activation have been demonstrated at the cellular level (Dana *et al*., 1998; Zhao *et al*., 2002; Shmelzer *et al*., 2003). Furthermore, recent studies have shown that the orchestration of low concentrations of AA produced by PLA_2 together with protein kinase C (PKC)-dependent phosphorylation promotes translocation of p47^{phox} and enhances ROS production by Nox2 (Shiose and Sumimoto, 2000; Peng *et al*., 2003).

In recent work, we described mechanisms for translocation of p47^{phox} (Ueyama *et al*., 2004) and isoform-specific translocation of Rac to the phagosome (Ueyama *et al*., 2005). To understand and clarify targeting of p67^{phox}, an essential cytoplasmic Nox2 activator that acts through Rac, we used AA as a stimulant and explored the adaptor functions of p40^{phox} and p47^{phox} in recruitment of p67^{phox} to membranes. In the present study, we show that p67^{phox} is not targeted to the membrane by itself but that it relies on diverse targeting and adaptor functions of p40^{phox} and p47^{phox} for its translocation to membranes. Furthermore, we examine the mechanism by which p40^{phox} acquires its function as a p67^{phox} "adaptor protein." We propose here that an intramolecular interaction between the PX and the PB1 domains of p40^{phox} in the resting state renders p40^{phox} inaccessible to bind PI(3)P and that upon stimulation the intramolecular interaction can be disrupted, enabling p40^{phox} to bind to PI(3)P-enriched membranes.

MATERIALS AND METHODS

Materials

Goat polyclonal antibody (Ab) against human p47^{phox} or p67^{phox} and rabbit polyclonal Ab against human p40^{phox} were described previously (Leto *et al*., 1991; Sathyamoorthy *et al*., 1997). Mouse monoclonal Ab against human p47^{phox} or p67^{phox} was from BD Biosciences (San Jose, CA). Rabbit polyclonal Ab against green fluorescent protein (GFP) or early endosome antigen-1 (EEA1) was from Clontech (Mountain View, CA) or from ABR-Affinity BioReagents (Golden, CO), respectively. Rabbit polyclonal Ab against glutathione *S*-transferase (GST) and mouse monoclonal Ab against $(His)_6$ were from Santa Cruz Biotechnology (Santa Cruz, CA) and GE Healthcare (Little Chalfont, Buckinghamshire, United Kingdom), respectively. AA was purchased from Doosan Serdary Research Laboratories (Kyungki-Do, Korea).

Cell Culture

RAW 264.7 macrophages (Ueyama *et al*., 2005) and COS-7 cells (American Type Culture Collection, Manassas, VA) were maintained in DMEM (Invitrogen, Carlsbad, CA) supplemented with 10% heat-inactivated fetal bovine serum (Invitrogen) and antibiotics (100 U/ml penicillin and 100 μg/ml streptomycin) at 37°C in 5% CO_2.

Construction of Plasmids

The pEGFP-C1 plasmids (Clontech) containing human p47^{phox}, p47^{phox}(W193R), p40^{phox}, p40^{phox}(PX; aa 1-167), p40^{phox}(PX:R105K), and p47^{phox}(R90K) were described previously (Ago *et al*., 2001, 2003; Ueyama *et al*., 2004). cDNA encoding p67^{phox} and p67^{phox}(ΔSH3, aa 1-457) were described previously (de Mendez *et al*., 1994; Ueyama *et al*., 2004), transferred into pEGFP-C1, and designated GFP-p67^{phox} and GFP-p67^{phox}(ΔSH3), respectively. The fragment encoding p67^{phox}(ΔAD, deletion of aa 199-212) was made by polymerase chain reaction (PCR) by using appropriate primers, transferred into pEGFP-C1, and designated GFP-p67^{phox}(ΔAD). The fragments encoding p47^{phox}, p47^{phox}(ΔPR; aa 1-359), and p40^{phox} were amplified by PCR, cloned into pIRES2-DsRed2, and designated p47^{phox}-IRES2-DsRed2, p47^{phox}(ΔPR)-IRES2-DsRed2, and p40^{phox}-IRES2-DsRed2, respectively. The fragments encoding p47^{phox} and GFP-p67^{phox}(ΔAD) were amplified by PCR, cloned into BglII and EcoRI sites of multiple cloning site of pIRES2-DsRed2 and BstXI and XbaI sites of pIRES2-DsRed2 in place of DsRed2, respectively, and designated p47^{phox}-IRES2-GFP-p67^{phox}(ΔAD). GFP-p40^{phox}(R105K), GFP-p67^{phox}(ΔAD:K355A), and p40^{phox}(D289A)-IRES2-DsRed2 were made using the QuikChange II XL site-directed mutagenesis kit protocol (Stratagene, La Jolla, CA). We confirmed that GFP-p47^{phox} and GFP-p67^{phox} support Nox2 activity at levels comparable with unfused, wild-type p47^{phox}, and p67^{phox} (data not shown).

To study the intramolecular binding of p40^{phox}, the DNA fragments encoding p40^{phox}(aa 1-229), p40^{phox}(aa 1-261), p40^{phox}(aa 1-284), p40^{phox}(aa 1-306), p40^{phox}(aa 1-317), and p40^{phox}(aa 1-328) were amplified by PCR, cloned into pEGFP-C1, and designated GFP-p40^{phox}(1-229), GFP-p40^{phox}(1-261), GFP-p40^{phox}(1-284), GFP-p40^{phox}(1-306), GFP-p40^{phox}(1-317), and GFP-p40^{phox}(1-328), respectively (Figure 9A). The DNA fragment encoding p40^{phox}(Δ318-328; deletion of aa 318-328) was amplified by PCR by using GFP-p40^{phox}(1-328) as a template with appropriate primers, cloned into pEGFP-C1, and designated GFP-p40^{phox}(Δ318-328). p40^{phox}(318-328:11A) in pEGFP-C1, in which residues 318-328 are replaced by 11 alanine residues, was made using GFP-p40^{phox} as a template by the QuikChange II XL site-directed mutagenesis kit. All modified expression vectors were sequenced to confirm their identities.

Immunoprecipitation and Immunoblotting

COS-7 cells were transfected using electroporation methods (Shirai *et al*., 1998). Forty-eight hours after the transfection, cells were lysed in homogenizing buffer in the presence of protease inhibitors (Ueyama *et al*., 2001) by sonication. The total cell lysates were centrifuged at 20,000 × *g* for 30 min at 4°C, the supernatants were incubated with the Ab (α-p47^{phox}, α-p67^{phox} or α-p40^{phox}, α-GFP) or control IgG (goat or rabbit; Santa Cruz Biotechnology, Santa Cruz, CA) for 2 h at 4°C and then with protein G-Sepharose 4B (GE Healthcare) for an additional 12 h at 4°C. The precipitates were washed three times, and the aliquots of precipitates were subjected to SDS-PAGE and followed by immunoblotting using primary Ab for α-p47^{phox}, α-p67^{phox}, α-p40^{phox}, or α-GFP (1/2000, room temperature [RT] for 2 h). Bound antibodies were detected with secondary antibody-horseradish peroxidase (HRP) conjugates (Jackson ImmunoResearch Laboratories, West Grove, PA) by using the ECL detection system (GE Healthcare).

Cell Imaging Studies

Fluorescently labeled (Alexa-568) and IgG-opsonized phagocytosis targets (BIgG) were prepared using 2-μm glass beads (Duke Scientific, Fremont, CA), as described previously (Larsen *et al*., 2002). In total, 1.0×10^5 RAW 264.7 cells were seeded on 35-mm glass bottom dishes (MatTek chambers; MatTek, Ashland, MA) and transfected using Superfect (QIAGEN, Valencia, CA). Twenty-four to 32 h after the transfection, the culture medium was replaced with Hanks' balanced salt solution $(HBSS)^{++}$ (Larsen *et al*., 2002). As a stimulant, $HBSS^{++}$ containing BIgG (five targets per cell) or $HBSS^{++}$ con-

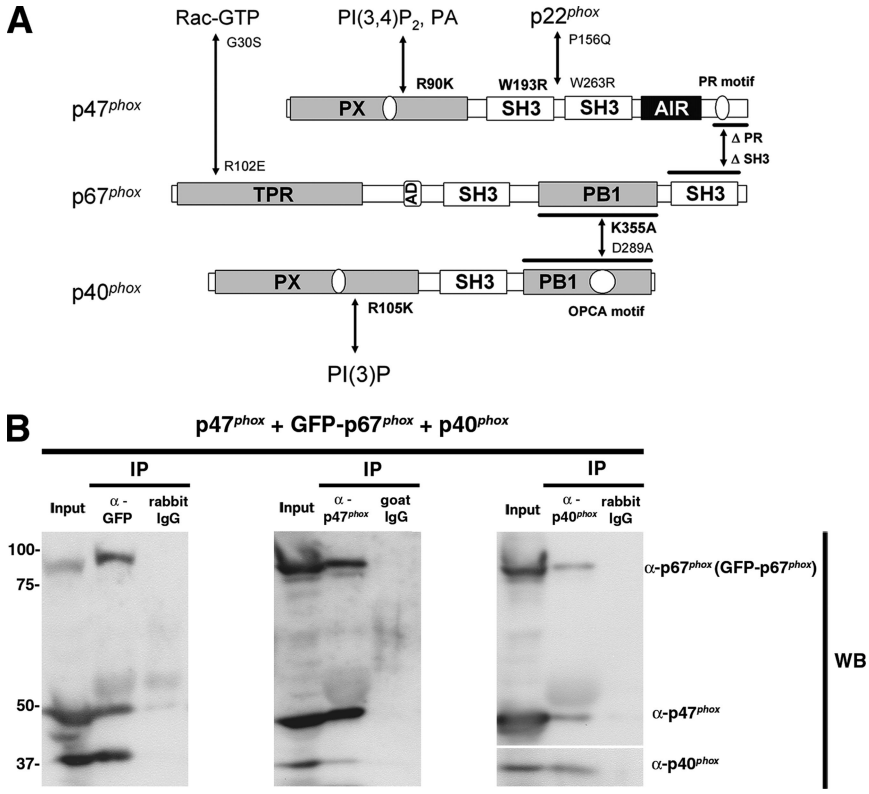

Figure 1. Phox proteins exist in a complex in resting COS-7 cells. (A) Schematic representation of structural domains and their interactions among p47^{phox}, p67^{phox}, and p40^{phox}. Additional interactions between Rac and p67^{phox}, p22^{phox} and p47^{phox}, PI(3,4)P_2, PA and the PX domain of p47^{phox}, and PI(3)P and the PX domain of p40^{phox} are also shown. AIR, autoinhibitory region; TPR, tetratricopeptide repeat; AD, activation domain; PB1, Phox and Bem1; OPCA, OPR-PC-AID. Mutations that disrupt these interactions are shown beside arrows; those used in the current study are in bold. (B) Supernatants from COS-7 cells expressing p47^{phox}, GFP-p67^{phox}, and p40^{phox} were immunoprecipitated by rabbit polyclonal antibodies against GFP or rabbit control IgG, goat polyclonal antibodies against p47^{phox} or goat control IgG, or rabbit polyclonal antibodies against p40^{phox} or rabbit control IgG and then immunoblotted with antibodies against p47^{phox} (monoclonal), p67^{phox} (monoclonal), and p40^{phox} (polyclonal). p47^{phox} and p40^{phox} are coimmunoprecipitated with GFP-p67^{phox} (left), GFP-p67^{phox} and p40^{phox} are coimmunoprecipitated with p47^{phox} (middle), and p47^{phox} and GFP-p67^{phox} are coimmunoprecipitated with p40^{phox} (right). Similar results were obtained in two independent experiments.

taining AA (indicated final concentrations) was added to each plate. Images were collected using an LSM 510 invert (Carl Zeiss, Thornwood, NY) confocal laser scanning fluorescence microscope with a heated stage and objective (40× oil or 63× oil) as described previously (Ueyama *et al.*, 2004). The images were collected at 5 s intervals for 5 min.

For immunocytochemical studies, cells (transfected or untransfected) were fixed with 4% paraformaldehyde in 0.1 M phosphate buffer (Ueyama *et al.*, 2001). After permeabilization, cells were stained using primary Ab (p40^{phox}, diluted 1/500; EEA-1, diluted 1/250) for 2 h at RT. Primary Abs were visualized by confocal microscopy using Alexa-488 or -594–conjugated anti-rabbit IgG (1/2000, 0.5 h at RT; Invitrogen).

All time-lapsed imaging experiments were performed in triplicate and were repeated in at least three independent transfection experiments ($n \geq 9$). All imaging experiments were very reproducible (≥80%), except for the experiment of GFP-p40^{phox} stimulated with BIgG (≤10%; Figure 2A and Supplemental Video 1).

In Vitro Binding Assay

The cDNA for the PCR-amplified PX domain of p40^{phox}(aa 1-167) was cloned into BamHI and EcoRI sites of pProEx-Htb (Invitrogen) and designated $(His)_6$-p40^{phox}(PX). Forward and reverse oligonucleotides for p40^{phox}(aa 307-317), p40^{phox}(aa 318-328), and p40^{phox}(aa 329-339) were annealed and cloned into the BamHI and EcoRI sites of pGEX-6P-1 and designated GST-p40^{phox}(307-317), GST-p40^{phox}(318-328), and GST-p40^{phox}(329-339), respectively. PCR-amplified fragments of p40^{phox}(SH3 domain; aa 170-229) and p40^{phox}(PB1 domain; aa 237-339) were cloned into the BamHI and EcoRI sites of pGEX-6P-1 and designated GST-p40^{phox}(SH3) and GST-p40^{phox}(237-339), respectively. All constructs were sequenced to confirm their identities. Tagged proteins were expressed in *Escherichia coli* strain BL21-CodonPlus (DE3)-RIL (Stratagene). When the bacteria reached an OD_{600} of ~0.2, protein expression was induced by 0.1 mM isopropyl β-D-thiogalactoside at 21°C for 16 h and purified using nickel-Agarose [Invitrogen; in the case of $(His)_6$-p40^{phox}(PX), the tagged protein was solubilized in 50 mM 3-[(3-cholamidopropyl)dimethylammonio]-1-propanesulfonate] or glutathione-Sepharose 4B (GE Healthcare). The purified $(His)_6$-p40^{phox}(PX) (500 nM) was mixed with each purified GST-tagged fragment of p40^{phox} (500 nM) in 500 μl of buffer (25 mM HEPES, 150 mM NaCl, and 2% fatty acid-free bovine serum albumin, pH 7.5). Glutathione-Sepharose 4B beads were added to the solution, rotated for 30 min at 4°C, and then washed three times with the same buffer. The material absorbed to beads was eluted with 10 mM glutathione, and the elutants were separated on a 15% SDS-polyacrylamide gel. Western blotting was performed using primary $(His)_6$ Ab and secondary Ab-HRP conjugates, and detected by the ECL detection system.

Online Supplemental Material

The supplemental time-lapsed photography shows the "kiss and run" fusion-like accumulation of GFP-p40^{phox} on phagosomes (Video 1; total time 330 s) and the transient accumulation of GFP-p40^{phox}(PX) on phagosomes by fusion of early endosomes and from a cytoplasmic pool of GFP-p40^{phox}(PX) (Video 2; total 310 s) during Fcγ receptor (FcγR)-mediated phagocytosis in RAW 264.7 cells. The supplemental time-lapsed photography shows translocation of GFP-p67^{phox}(ΔAD) both to early endosomes and to the plasma membrane (Video 3; total time 150 s) after AA stimulation in RAW 264.7 cells coexpressing p40^{phox} and p47^{phox}.

RESULTS

Accumulation of p40^{phox}(PX) at the Phagosome during FcγR-mediated Phagocytosis

Although a recent study reported that p40^{phox} and p67^{phox} exist as a heterodimer in the resting state and that the p47^{phox}-containing ternary complex forms only after cell activation (Brown *et al.*, 2003), most other studies to date indicate that the phox proteins exist as a stable 1:1:1 ternary cytoplasmic complex (p47^{phox}-p67^{phox}-p40^{phox}) in their dephosphorylated state even without cell stimulation (Figure 1A; Bolscher *et al.*, 1989; Rotrosen and Leto, 1990; Lapouge *et al.*, 2002; Kuribayashi *et al.*, 2002). We examined ternary complex formation by using GFP-p67^{phox} coexpressed with p47^{phox} and p40^{phox} in COS-7 cells and confirmed that all three proteins exist at least partially in a complex that could be detected by immunoprecipitation with antibodies against any of these components (Figure 1B). Furthermore, we examined ROS production using GFP-p67^{phox} or p67^{phox} plus p47^{phox} and Nox2 in human embryonic kidney 293 and COS-7 cell models, and confirmed that GFP-p67^{phox} supports Nox2 activity at levels comparable with the unfused, wild-type p67^{phox} (data not shown). These results indicate that GFP-p67^{phox} behaves like wild-type p67^{phox}, at least with regard to its interactions and assembly with other phox

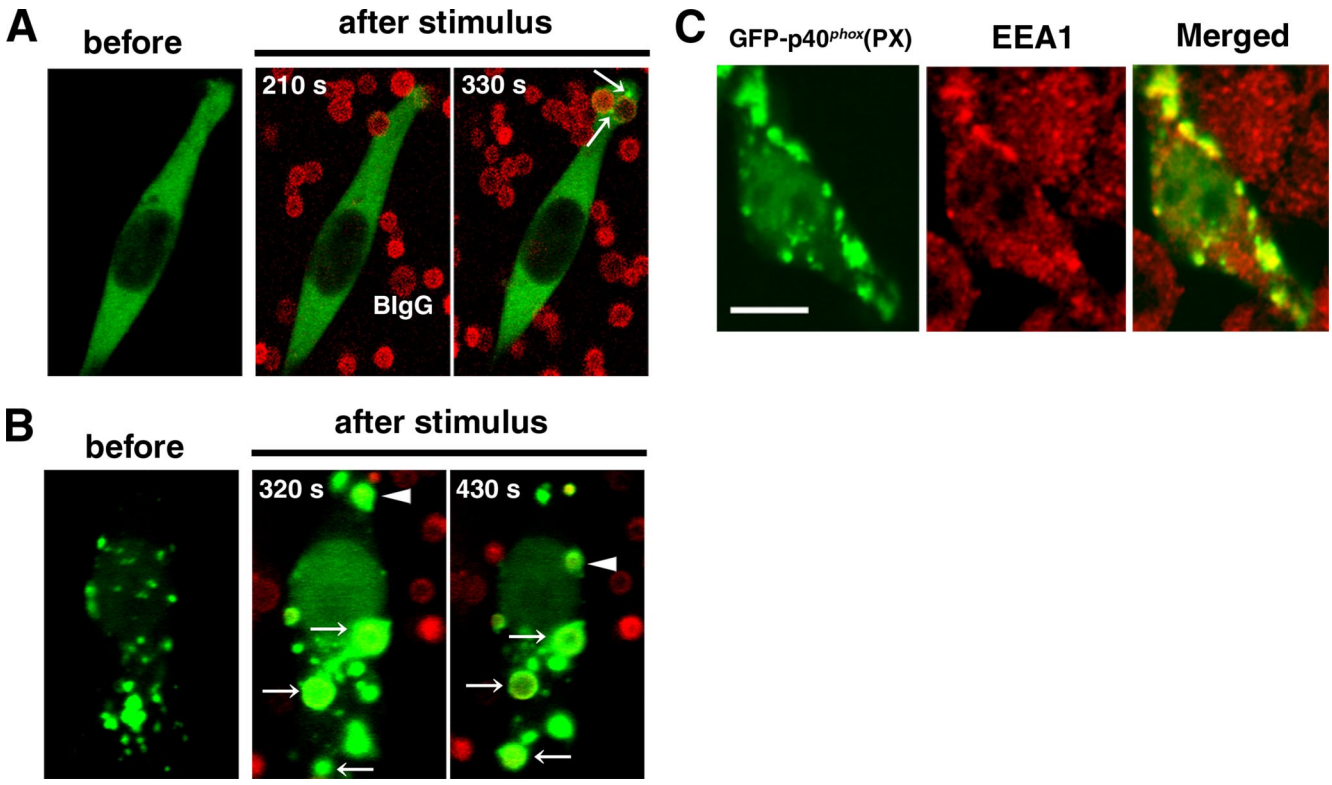

Figure 2. Accumulation of GFP-p40^{phox}(PX) and full-length GFP-p40^{phox} on membranes during FcγR-mediated phagocytosis in RAW 264.7 cells. (A) During FcγR-mediated phagocytosis, transient vesicular accumulation of GFP-p40^{phox} (arrows) is observed occasionally, which fuses with newly forming phagosomes. Time-lapsed photography of this process is available in Supplemental Video 1. BIgG, Alexa-568 labeled– and IgG-opsonized 2-μm glass beads. Addition of BIgG occurs at time 0. Representative of n ≥ 30. (B) GFP-p40^{phox}(PX) is localized prominently on vesicular structures in the cytoplasm, which accumulates on phagosomes (arrows and arrowheads) during FcγR-mediated phagocytosis after phagosome sealing. Time-lapsed photography is available in Supplemental Video 2. Representative of n ≥ 9. (C) Vesicular structures containing GFP-p40^{phox}(PX) in the cytoplasm are reactive with antibodies against EEA-1, a marker of early endosomes in RAW 264.7 cells. Bar, 10 μm. Representative of n ≥ 6.

proteins and its ability to support ROS production in the Nox2 system. Therefore, we used GFP-p67^{phox} to monitor its interactions with other oxidase components in intact cells.

Because we described the mechanism of GFP-p47^{phox} accumulation on phagosomal cups and phagosomes during FcγR-mediated phagocytosis (Ueyama *et al*., 2004), the present study focused on p40^{phox}. GFP-p40^{phox} is detected diffusely throughout the cytoplasm of resting RAW 264.7 cells (Figure 2A). During FcγR-mediated phagocytosis, the accumulation of GFP-p40^{phox} on newly forming phagosomes occurs as a kiss and run phenomenon, in which a transient fusion of GFP-p40^{phox} is observed between phagosomes and endosomes without showing much evidence of complete intermixing of their membranes (Duclos *et al*., 2000). This phenomenon is not observed constantly (≤10%), but it occurred only occasionally when followed by time-lapsed photography (Figure 2A and Supplemental Video 1). We then used GFP-p40^{phox}(PX) for further studies, because it was reported to bind specifically to PI(3)P. Consistent with a previous report (Ellson *et al*., 2001a), GFP-p40^{phox}(PX) is localized faintly in the cytoplasm and predominantly on vesicular structures (Figure 2B), which could be colabeled with antibodies against early endosomal antigen (EEA)-1 (Figure 2C), a marker of the early endosome that is enriched in PI(3)P (Gillooly *et al*., 2000) (Figure 2B). The vesicular structures and free-form of GFP-p40^{phox}(PX) seems to fuse readily with phagosomes in later stages of FcγR-mediated phagocytosis, after the phagosome is sealed (Figure 2B and Supplemental Video 2). The fusion of early endosomes, as detected by GFP fluorescence, resembles the same kiss and run pattern (transient interaction); however, the GFP-p40^{phox}(PX) fluorescence seems to reflect significant amounts membrane material fusing with the phagosomes (Supplemental Video 2). This accumulation of GFP-p40^{phox}(PX) on the phagosome persists longer on phagosomes (>100 s) than observed with GFP-p47^{phox}, which starts accumulating before phagosome sealing (on phagosomal cups) and is observed on phagosomal cups and retained on phagosomes for 67 ± 7 s (Ueyama *et al*., 2004). Accumulation of GFP-p67^{phox} on phagosomes was not evident in RAW 264.7 during FcγR-mediated phagocytosis, perhaps reflecting low levels of expression of the endogenous phox proteins (data not shown). However, GFP-p67^{phox} accumulated at phagosomal cups and phagosomes after coexpression with p47^{phox} (data not shown). The differences in localization patterns between GFP fusion proteins of full-length p40^{phox} and its isolated PX domain suggest that the PX domain of p40^{phox} is masked or is otherwise maintained in a state that is relatively inaccessible to early endosomes or PI(3)P-enriched phagosomes. The differences in localization between p40^{phox} and p47^{phox} fusions proteins suggest that the two proteins are targeted to phagosomes by distinctly different signals.

Translocation of p40^{phox} and p47^{phox}, but Not p67^{phox}, to Membranes after AA Stimulation

To examine the mechanism by which p40^{phox} acquires the capacity to bind PI(3)P, we explored the effects of cell stimulation by phorbol 12-myristate 13-acetate (PMA), *N*-formyl-

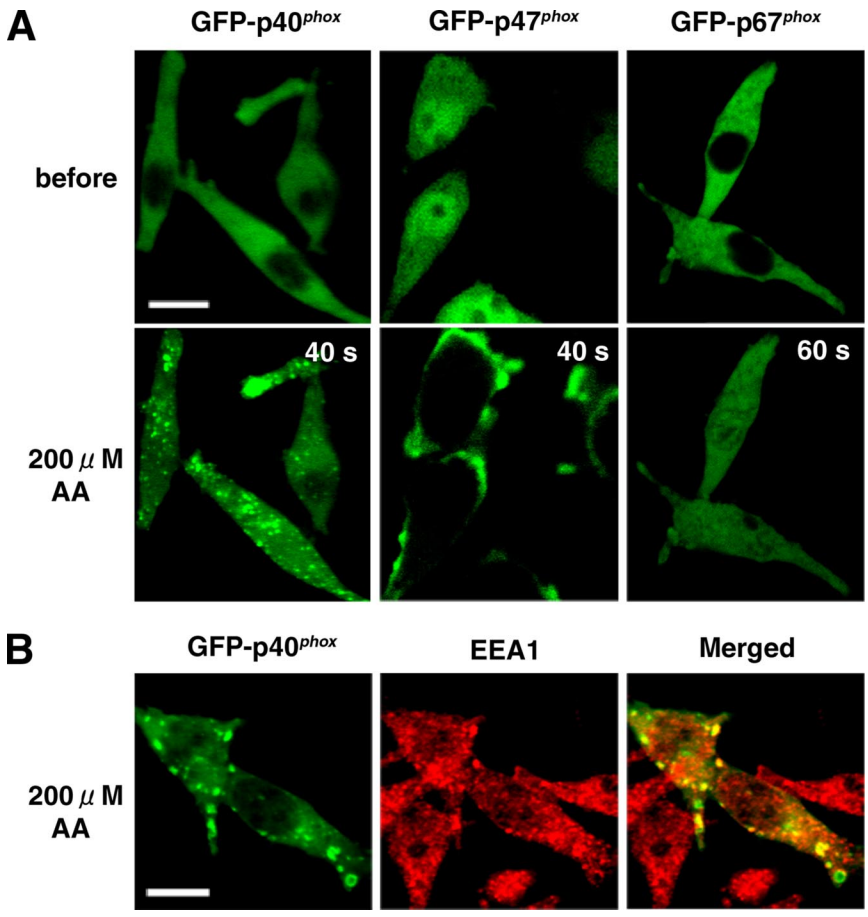

Figure 3. AA-stimulated translocation of GFP-p40^{phox} and GFP-p47^{phox}, but not GFP-p67^{phox}, to the membrane in RAW 264.7 cells. (A) Left, AA triggers GFP-p40^{phox} translocation to vesicular structures in the cytoplasm. (A) Middle, AA stimulates GFP-p47^{phox} translocation to the plasma membrane. (A) Right, GFP-p67^{phox} shows no significant translocation to membranes. AA was added at time 0. Bar, 10 μm. Representative of n $\geq$ 9. (B) Vesicular structures in the cytoplasm containing GFP-p40^{phox} are labeled with antibodies against EEA-1, a marker of early endosomes. Bar, 10 μm. Representative of n $\geq$ 6.

L-methionyl-L-leucyl-L-phenylalanine (fMLP), or AA. Among these stimulants, only AA can induce any detectable translocation of GFP-p40^{phox} in our real-time confocal microscopy system, which shows that GFP-p40^{phox} translocates to vesicular structures in the cytoplasm (Figure 3A, left) that are colabeled with antibodies against EEA-1 (Figure 3B). The same translocation pattern of AA-induced GFP-p40^{phox} translocation is observed using a C-terminally tagged GFP fusion with p40^{phox}, p40^{phox}-GFP (data not shown). In contrast, GFP-p47^{phox} translocates to the plasma membrane after cell stimulation by AA (Figure 3A, middle), whereas GFP-p67^{phox} shows no translocation to any membranes after treatments by any of these three stimulants (Figure 3A, right). These data suggest that AA induces conformational changes in p40^{phox} that render the PX domain accessible to bind to early endosomes, as occurs in AA-treated p47^{phox} to expose its SH3 domains to bind to p22^{phox} (Shiose and Sumimoto, 2000; Zhao *et al*., 2002). It is intriguing that GFP-p40^{phox} and GFP-p47^{phox}, but not GFP-p67^{phox}, have the ability to bind to the membrane only after AA stimulation, which likely induces conformational change in both proteins.

There are reports that phosphorylation occurs within p40^{phox} at Thr154 and Ser315 (Bouin *et al*., 1998) and that phosphorylation of Thr154, but not Ser315, inhibits Nox2 activation (Lopes *et al*., 2004). Therefore, we made mutants of GFP-p40^{phox} that could not be phosphorylated [GFP-p40^{phox}(T154A) and GFP-p40^{phox}(S315A)] or mimic the phosphorylated states [GFP-p40^{phox}(T154D) and GFP-p40^{phox}(S315D)]. However, these mutants are localized throughout the cytoplasm and seem to translocate normally to early endosomes after AA stimulation, like GFP-p40^{phox} (data not shown).

Function of PX Domains of p40^{phox} and p47^{phox} for Their Translocation

We then explored the translocation mechanisms of p40^{phox} and p47^{phox} by examining the effects of mutating their PX domains. GFP-p40^{phox}(PX:R105K), which loses its capacity to bind PI(3)P (Ago *et al*., 2001), shows no vesicular localization pattern, nor does it translocate to early endosomes after AA stimulation (Figure 4A). GFP-p40^{phox}(R105K) also shows no translocation to the early endosome after AA stimulation (Figure 4B). These observations indicate that translocation of p40^{phox} to early endosomes requires binding of the PX domain to PI(3)P.

In the case of p47^{phox}, GFP-p47^{phox}(R90K), which loses its capacity to bind PI(3,4)P_2 (Ago *et al*., 2003), shows no translocation to the plasma membrane by AA (Figure 4C). GFP-p47^{phox}(W193R), which cannot translocate to the phagosome to bind to proline-rich (PR) motif of p22^{phox} (Ueyama *et al*., 2004) nor produce ROS (Sumimoto *et al*., 1996; de Mendez *et al*., 1997), also shows no translocation to the plasma membrane after AA stimulation (Figure 4D). Together, these data indicate that translocation of p47^{phox} to the plasma membrane after AA stimulation requires both the binding of the PX domain to PI(3,4)P_2 and the SH3 domain interaction with p22^{phox}.

Targeting of p67^{phox} to Early Endosomes or to the Plasma Membrane by Coexpressed Carrier Proteins, p40^{phox} or p47^{phox}

To clarify the function of p40^{phox} as a potential membrane "adaptor protein" for p67^{phox}, we expressed GFP-p67^{phox} and

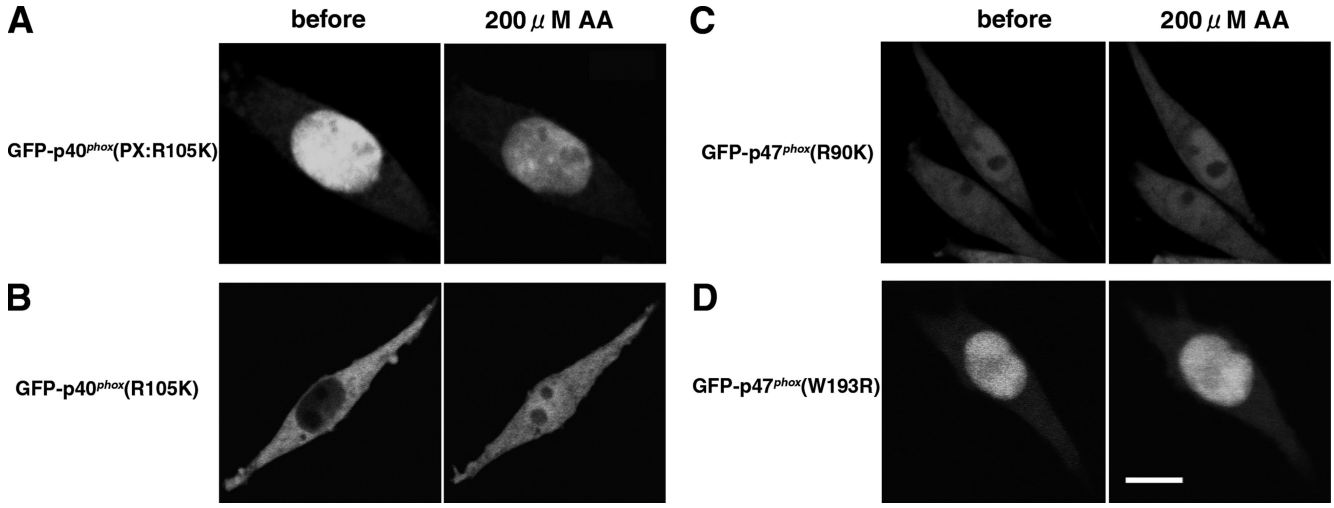

Figure 4. Requirement of phosphatidylinositol phosphate-specific binding of PX domains for translocation of $p40^{phox}$ and $p47^{phox}$ in AA-stimulated RAW 264.7 cells. (A) GFP-$p40^{phox}$(PX:R105K), which loses the capacity for binding PI(3)P, shows no vesicular localization pattern nor translocation to early endosomes. Representative of $n \geq 9$. (B) GFP-$p40^{phox}$(R105K) shows no translocation to early endosomes. Representative of $n \geq 9$. (C) GFP-$p47^{phox}$(R90K), which loses the capacity for binding $PI(3,4)P_2$, shows no translocation to the plasma membrane. Representative of $n \geq 9$. (D) GFP-$p47^{phox}$(W193R), which cannot bind to $p22^{phox}$, shows no translocation to the plasma membrane. Bar, 10 μm. Representative of $n \geq 9$.

$p40^{phox}$-IRES2-DsRed2, which identifies transfected cells expressing wild-type $p40^{phox}$ by DsRed2 fluorescence. When GFP-$p67^{phox}$ and $p40^{phox}$-IRES2-DsRed2 are cotransfected into RAW 264.7 cells, we cannot easily detect cells coexpress-

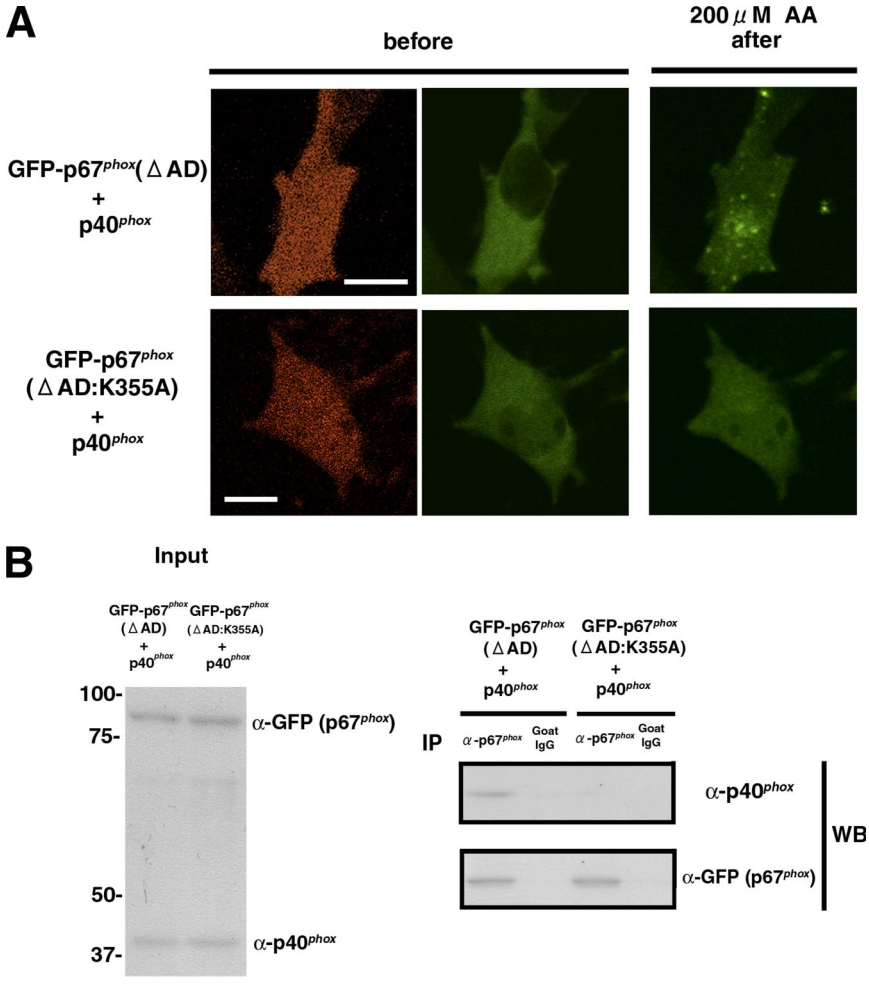

Figure 5. Targeting of GFP-$p67^{phox}$(ΔAD) to early endosomes by coexpression of $p40^{phox}$ in RAW 264.7 cells. (A) Top, coexpression of GFP-$p67^{phox}$(ΔAD) and $p40^{phox}$-IRES2-DsRed2 enables GFP-$p67^{phox}$(ΔAD) translocation to vesicular structures. DsRed2 fluorescence (left) identifies cells expressing $p40^{phox}$. Bar, 10 μm. Representative of $n \geq 9$. (A) Bottom, GFP-$p67^{phox}$(ΔAD:K355A) shows no translocation to vesicular structures when coexpressed with $p40^{phox}$-IRES2-DsRed2. DsRed2 fluorescence (left) identifies cells expressing $p40^{phox}$. Bar, 10 μm. Representative of $n \geq 9$. (B) Supernatants from COS-7 cells expressing $p40^{phox}$ and GFP-$p67^{phox}$(ΔAD) or GFP-$p67^{phox}$(ΔAD:K355A) were immunoprecipitated by goat polyclonal antibodies against $p67^{phox}$ or goat control IgG and immunoblotted with rabbit polyclonal antibodies against $p40^{phox}$ and GFP. $p40^{phox}$ is coimmunoprecipitated with GFP-$p67^{phox}$(ΔAD) but not GFP-$p67^{phox}$(ΔAD:K355A). Similar results were obtained in two independent experiments.

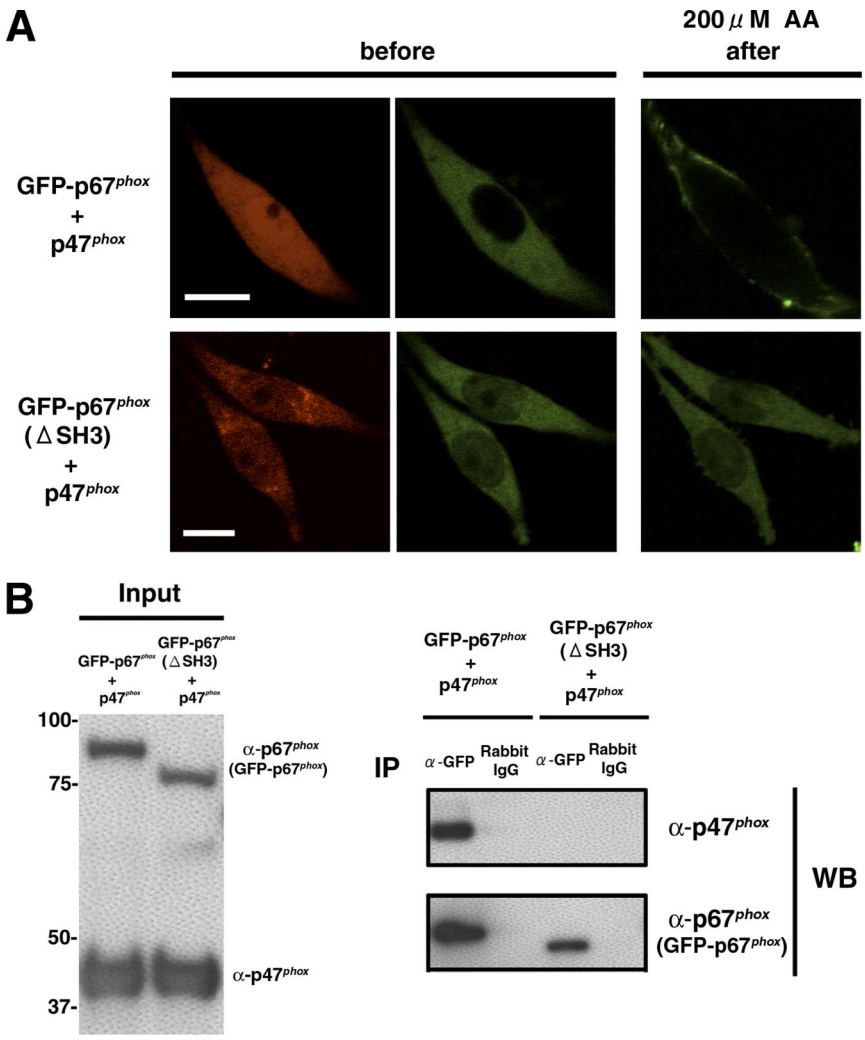

Figure 6. Targeting of GFP-p67^{phox} to the plasma membrane by coexpression of p47^{phox} in RAW 264.7 cells. (A) Top, coexpression of GFP-p67^{phox} and p47^{phox}-IRES2-DsRed2 enables GFP-p67^{phox} translocation to the plasma membrane. DsRed2 fluorescence (left) shows cells expressing p47^{phox}. Bar, 10 μm. Representative of n $\geq$ 9. (A) Bottom, GFP-p67^{phox}(ΔSH3) shows no translocation to the plasma membrane when coexpressed with p47^{phox}-IRES2-DsRed2. DsRed2 fluorescence (left) shows cells expressing p47^{phox}. Bar, 10 μm. Representative of n $\geq$ 9. (B) Supernatants from COS-7 cells expressing p47^{phox} and GFP-p67^{phox} or GFP-p67^{phox}(ΔSH3) were immunoprecipitated by rabbit polyclonal antibodies against GFP or control rabbit IgG and then immunoblotted with goat polyclonal antibodies against p47^{phox} and p67^{phox}. p47^{phox} is coimmunoprecipitaed with GFP-p67^{phox}, but not GFP-p67^{phox}(ΔSH3). Similar results were obtained in two independent experiments.

ing these products. We speculate that overexpression of p67^{phox} and p40^{phox} may be too toxic to cells due to the enhanced production of ROS. Therefore, further studies were performed using p67^{phox}(ΔAD), which cannot support ROS production (Han *et al*., 1998). In RAW 264.7 cells coexpressing GFP-p67^{phox}(ΔAD) and p40^{phox}-IRES2-DsRed2, GFP-p67^{phox}(ΔAD) translocates to vesicular structures (Figure 5A, top). However, in cells coexpressing p40^{phox}-IRES2-DsRed2 and GFP-p67^{phox}(ΔAD:K355A), which does not bind p40^{phox} (Kuribayashi *et al*., 2002), GFP-p67^{phox}(ΔAD:K355A) does not translocate to the vesicular structures (Figure 5A, bottom). This result is further confirmed by complementary experiments using GFP-p67^{phox}(ΔAD) and p40^{phox}(D289A)-IRES2-DsRed2, which does not interact with p67^{phox} (Kuribayashi *et al*., 2002). In cells coexpressing GFP-p67^{phox}(ΔAD) and p40^{phox}(D289A)-IRES2-DsRed2, GFP-p67^{phox}(ΔAD) shows no translocation to the vesicular structure (data not shown). The interaction between p40^{phox} and GFP-p67^{phox}(ΔAD), but not GFP-p67^{phox}(ΔAD:K355A), is confirmed by immunoprecipitation experiments (Figure 5B).

In the case where p47^{phox} is used as a membrane adaptor protein for p67^{phox}, GFP-p67^{phox} translocates to the plasma membrane in RAW 264.7 cells (Figure 6A, top). However, in cells coexpressing p47^{phox}-IRES2-DsRed2 and GFP-p67^{phox}(ΔSH3), which disrupts the interaction with p47^{phox} (de Mendez *et al*., 1994), no GFP-p67^{phox}(ΔSH3) translocation to the plasma membrane is seen (Figure 6A, bottom). This result was further confirmed by complementary experiment using GFP-p67^{phox} and p47^{phox}(ΔPR)-IRES2-DsRed2, which also disrupts the interaction with p67^{phox} (Kami *et al*., 2002; Massenet *et al*., 2005). In the cells coexpressing GFP-p67^{phox} and p47^{phox}(ΔPR)-IRES2-DsRed2, GFP-p67^{phox} shows no the translocation to the plasma membrane (data not shown). The interaction between p47^{phox} and GFP-p67^{phox}, but not GFP-p47^{phox}(ΔSH3), is confirmed in immunoprecipitation experiments (Figure 6B). These data indicate that both p40^{phox} and p47^{phox} can function as adaptors of p67^{phox} to translocate p67^{phox} to the early endosome and to the plasma membrane, respectively.

Because there are a few studies reporting weak interactions between p47^{phox} and p40^{phox} detected in vitro and in the yeast two-hybrid system (Sathyamoorthy *et al*., 1997; Grizot *et al*., 2001; Lapouge *et al*., 2002; Massenet *et al*., 2005), we examined the effect of this interaction on membrane translocation of p47^{phox} and p40^{phox}. Coexpression of p40^{phox}-IRES2-DsRed2 does not influence the translocation of GFP-p47^{phox} to the plasma membrane in RAW 264.7 cells (Figure 7A, top). Furthermore, coexpression of p47^{phox}-IRES2-DsRed2 does not influence the translocation of GFP-p40^{phox} to the vesicular structures (Figure 7A, bottom). Finally, no apparent interaction is detected between p40^{phox} and p47^{phox} (Figure 7B) by immunoprecipitation experiments. These data indicate that the interaction between p40^{phox} and p47^{phox} is

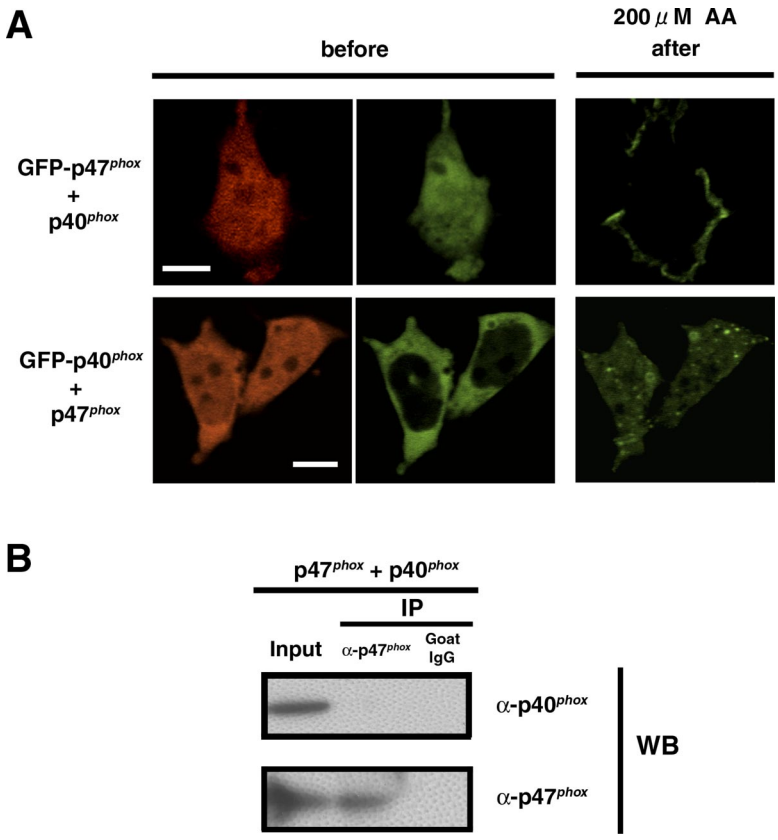

Figure 7. Independent membrane targeting of p40^{phox} and p47^{phox} in RAW 264.7 cells. (A) Top, p40^{phox} does not influence GFP-p47^{phox} targeting to the plasma membrane after AA stimulation. DsRed2 fluorescence (left) shows cells expressing p40^{phox}. Bar, 10 μm. Representative of n $\geq$ 9. (A) Bottom, p47^{phox} does not influence the GFP-p40^{phox} targeting to vesicular structures after AA stimulation. DsRed2 fluorescence (left) shows cells expressing p47^{phox}. Bar, 10 μm. Representative of n $\geq$ 9. (C) Supernatants from COS-7 cells expressing p40^{phox} and p47^{phox} were immunoprecipitated by goat polyclonal antibodies against p47^{phox} or goat control IgG and were immunoblotted with rabbit polyclonal antibodies against p40^{phox} and goat polyclonal antibodies against p47^{phox}. p40^{phox} is not coimmunoprecipitated with p47^{phox}. Similar results were obtained in two independent experiments.

below detectable levels and does not seem to be a factor in membrane targeting of these proteins in this system.

Finally, we examined the case where all of three phox proteins are overexpressed in RAW 264.7 cells using p47^{phox}-IRES2-GFP-p67^{phox}(ΔAD) and p40^{phox}-IRES2-DsRed2, which identifies transfected cells expressing wild-type p47^{phox} and GFP-p67^{phox}(ΔAD) by GFP fluorescence and wild-type p40^{phox} by DsRed2 fluorescence. In the RAW 264.7 cells coexpressing GFP-p67^{phox}(ΔAD), p47^{phox}, and p40^{phox}, GFP-p67^{phox}(ΔAD) translocates both to the plasma membrane and to vesicular structures after AA stimulation (Figure 8A and Supplemental Video 3). Expression of all three phox proteins by the internal ribosome entry site (IRES) plasmids is confirmed by Western blotting by using COS-7 cells (Figure 8B).

PB1 Domain of p40^{phox} Masks the PX Domain of p40^{phox}

It has been suggested that p47^{phox} exists in the cytoplasm in the resting state because of two intramolecular interactions

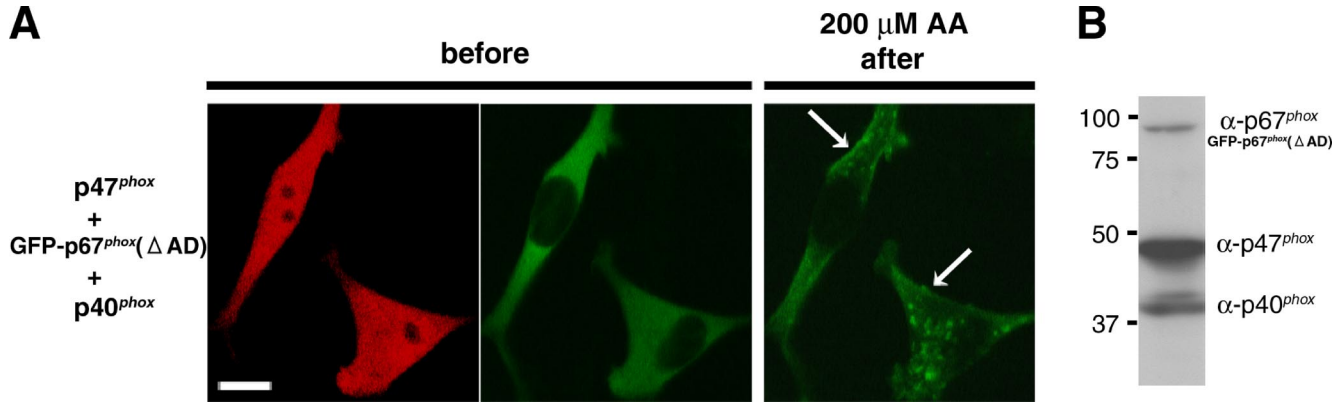

Figure 8. Targeting of GFP-p67^{phox}(ΔAD) both to early endosomes and to the plasma membrane by coexpression of p40^{phox} and p47^{phox} in RAW 264.7 cells. (A) Cotransfection of p47^{phox}-IRES2-GFP-p67^{phox}(ΔAD) and p40^{phox}-IRES2-DsRed2 enables GFP-p67^{phox}(ΔAD) translocation both to vesicular structures and to the plasma membrane (arrows). DsRed2 fluorescence (left) shows cells expressing p40^{phox}, and GFP fluorescence shows cells expressing p47 ^{phox} and GFP-p67^{phox}(ΔAD) (middle). Time-lapsed photography is available in supplemental Video 3. Bar, 10 μm. Representative of n $\geq$ 9. (B) Supernatants from COS-7 cells expressing p47^{phox} and GFP-p67^{phox}(ΔAD) by p47^{phox}-IRES2-GFP-p67^{phox}(ΔAD) and p40^{phox} by p40^{phox}-IRES2-DeRed2 were immunoblotted with antibodies against p47^{phox}, p67^{phox}, and p40^{phox}. Expression of all three phox proteins by IRES plasmids is confirmed. Similar results were obtained in two independent experiments.

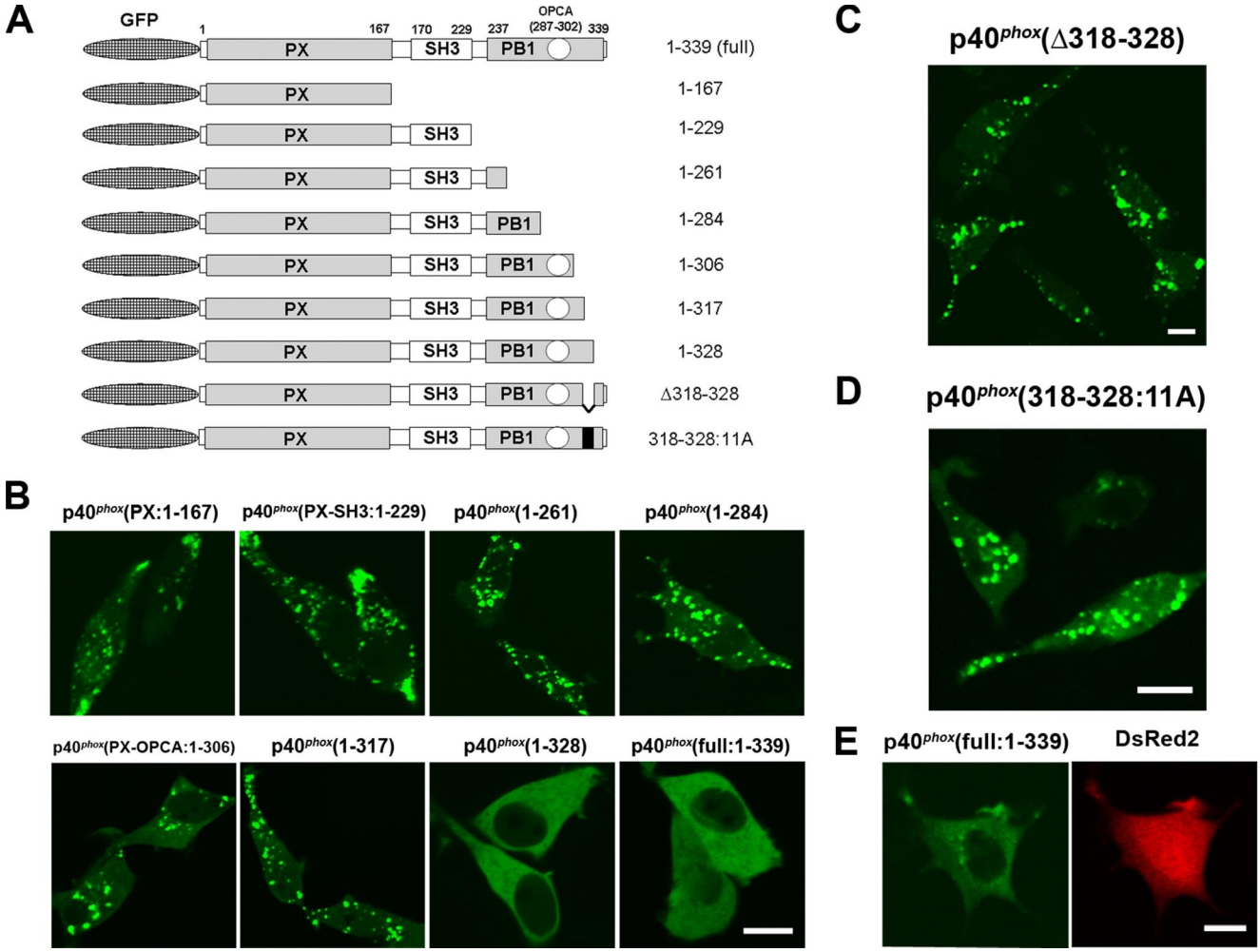

Figure 9. Inhibitory effects of the p40^{phox} PB1 domain (residues 318-328) in PX domain-mediated targeting of p40^{phox} to vesicular structures in RAW 264.7 cells. (A) Structure of GFP-tagged p40^{phox} constructs used in the present study. (B) GFP-p40^{phox}(PX), GFP-p40^{phox}(1-229), GFP-p40^{phox}(1-261), GFP-p40^{phox}(1-284), GFP-p40^{phox}(1-306), and GFP-p40^{phox}(1-317) are localized on vesicular structures. In contrast, full-length GFP-p40^{phox}(1–339) and GFP-p40^{phox}(1-328) remain localized in the cytoplasm. Bar, 10 μm. Representative of n $\geq$ 6. (C) GFP-p40^{phox}(Δ318-328) is localized on vesicular structures. Bar, 10 μm. Representative of n $\geq$ 6. (D) GFP-p40^{phox}(318-328:11A) is localized on vesicular structures. Bar, 10 μm. Representative of n $\geq$ 6. (E) Exogenously expressed wild-type p40^{phox} is primarily detected by immunofluorescence in the cytoplasm in COS-7 cells (left). p40^{phox} expressing cell is detected by DsRed2 fluorescence by using p40^{phox}-IRES2-DsRed2 plasmid (right). Bar, 10 μm. Representative of n $\geq$ 6.

masking both the N- and C-terminal SH3 domains and the PX domain (Hiroaki *et al*., 2001; Karathanassis *et al*., 2002; Groemping *et al*., 2003; Durand *et al*., 2006). When phagocytes are activated after cell stimulation, the autoinhibitory region (AIR) (aa 286-340) is phosphorylated, thereby disrupting the intramolecular interactions and rendering both SH3 domains and the PX domain accessible to bind p22^{phox} and membrane lipids, respectively (Karathanassis *et al*., 2002; Ago *et al*., 2003; Groemping *et al*., 2003). It was reported that the interaction between the PR motif in the PX domain and the C-terminal SH3 domain of p47^{phox} (Hiroaki *et al*., 2001). p40^{phox} also has a PR motif in the PX domain and one SH3 domain, which have the possibility of interacting each other. Therefore, we examined this possibility using purified (His)$_6$-p40^{phox}(PX) and GST-p40^{phox}(SH3) in in vitro pull-down binding assays. However, we did not detect binding between these two proteins (data not shown). This result is consistent with crystallographic data on p40^{phox}(PX) showing that the PR motif in the PX domain of p40^{phox} is buried within the PX domain, although this study was performed using the lipid-bound form of p40^{phox}(PX) (Bravo *et al*., 2001).

Then, we examined other regions within p40^{phox} that might interact with its own PX domain, by using serially deleted mutants of GFP-p40^{phox} expressed in RAW 264.7 cells. Among the various C-terminal deletions of GFP-p40^{phox}, GFP-p40^{phox}(1-328) loses the punctate localization on early endosomes, as seen with full-length GFP-p40^{phox} (Figure 9B). GFP-p40^{phox}(Δ318-328) and GFP-p40^{phox}(318-328:11A) are localized at vesicular structures in the cytoplasm (Figure 9, C and D). The cytoplasmic localization of wild-type p40^{phox} is confirmed by indirect immunofluorescence of COS-7 cells transfected with wild-type p40^{phox} (Figure 9E). To examine further, we used in vitro pull-down assays between purified (His)$_6$-p40^{phox}(PX) and various forms of purified GST-tagged proteins. We could not detect interactions between (His)$_6$-p40^{phox}(PX) and GST-p40^{phox}(307-317), GST-p40^{phox}(318-328), GST-p40^{phox}(329-339), or GST alone; however, (His)$_6$-p40^{phox}(PX) interacts strongly with GST-p40^{phox}(PB1:237-339) (Figure 10). These results suggested that

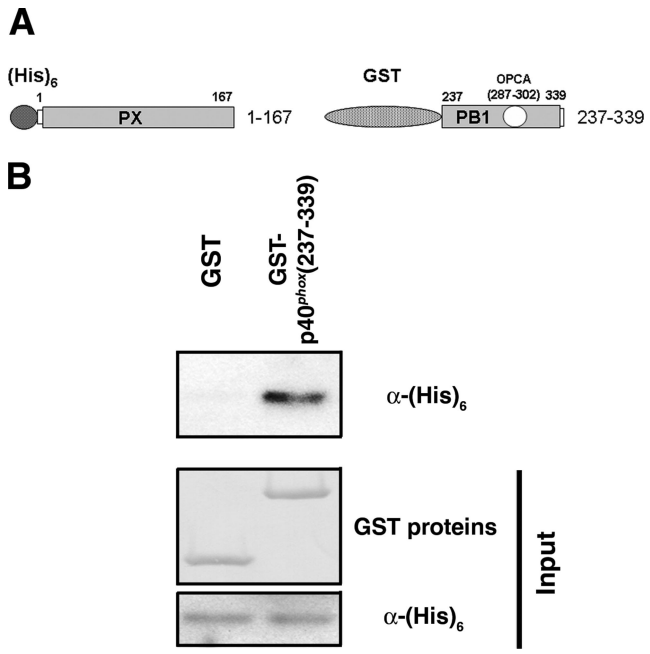

Figure 10. Interaction of PX domain and PB1 domain of p40^{phox}. (A) Structure of $(His)_6$-tagged PX domain (1–167) of p40^{phox} and GST-tagged PBI domain (237–339) of p40^{phox} constructs used in pull-down assays. (B) Top blot, purified GST-p40^{phox}(PBI: 237–339), but not GST, interacts with $(His)_6$-p40^{phox}(PX) in GST-based pull-down assays. Middle and bottom blots, comparable amounts of input proteins are confirmed by Ponsceau S staining (GST proteins) and by $(His)_6$ blotting [$(His)_6$-p40^{phox}(PX)], respectively. Representative of three independent experiments.

the PB1 domain of p40^{phox} masks the PX domain of p40^{phox}, making this domain inaccessible to bind to early endosomes in the absence of AA stimulation (Figure 11).

DISCUSSION

In this study, we propose that both p40^{phox} and p47^{phox} function as regulated carrier or adaptor proteins of p67^{phox} through distinct membrane-targeting mechanisms during NADPH oxidase assembly. We reported that p47^{phox} accumulates transiently on phagocytic cups and mature phagosomes during FcγR-mediated phagocytosis (Ueyama *et al.*, 2004), consistent with earlier studies showing p47^{phox} and p67^{phox} associate with both nascent and mature phagosomes in neutrophils and neutrophil-like PLB-985 cells (Allen *et al.*, 1999; van Bruggen *et al.*, 2004). The present study shows that GFP-p40^{phox} also transiently associates on phagosomes, although this targeting is initiated at later stages after phagosome sealing. This accumulation is even more apparent with GFP-p40^{phox}(PX), suggesting the PX domain of p40^{phox} is masked or otherwise inhibited from interacting with membranes in the context of the full-length protein, because the isolated PX domain binds readily to PI(3)P-enriched endosome-like vesicles even before phagocytic stimulation. Finally, we show that AA has dramatic affects in unmasking the PX domain, thereby enabling p40^{phox} to bind these vesicles along with p67^{phox}. We suggest two mechanisms for the targeting p40^{phox} to phagosomes during FcγR-mediated phagocytosis: 1) p40^{phox} can bind initially to PI(3)P-enriched early endosomes, followed by their fusion to phagosomes, and/or 2) p40^{phox} can target directly to phagosomes, where PI(3)P is transiently produced during phagosytosis (Ellson *et al.*, 2001a; Gillooly *et al.*, 2001). Because the cytosolic phox proteins exist as a ternary complex (Kuribayashi *et al.*, 2002; Lapouge *et al.*, 2002), we propose a model for Nox2 complex assembly involving these spatiotemporal factors during the FcγR-mediated respiratory burst (Figure 11): 1) in early stages, before phagosome sealing, p47^{phox} functions as the predominant carrier, mediating translocation of the ternary complex to newly forming phagosomes, 2) in later stages

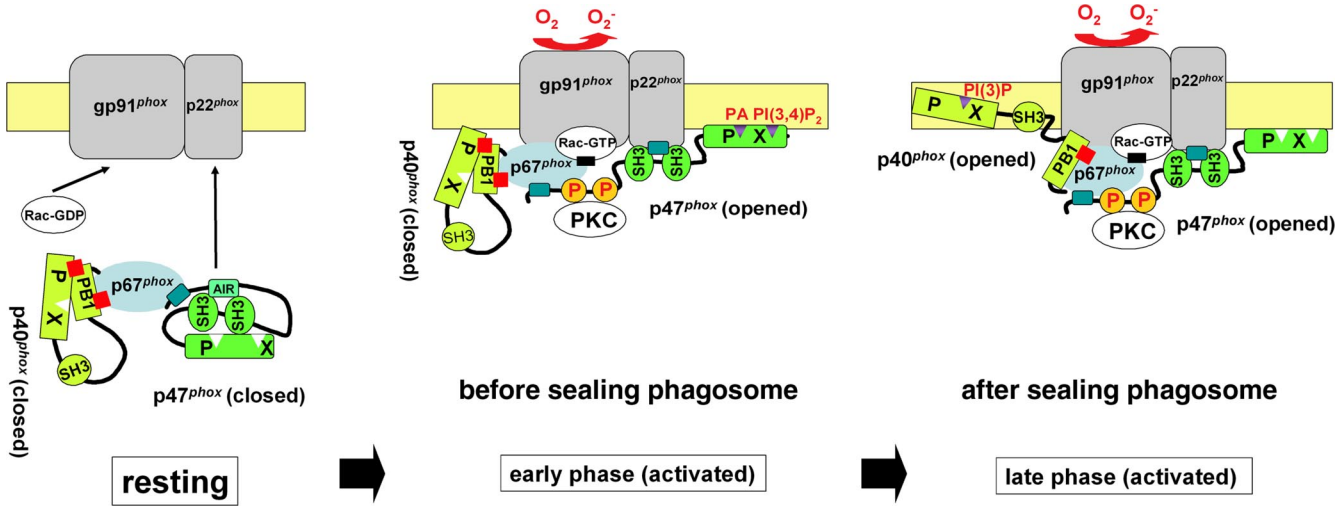

Figure 11. Model of activation and assembly of Nox2 system during phagocytosis. In the resting state, the ternary complex of p47^{phox}, p67^{phox}, and p40^{phox} is in the cytoplasm. p47^{phox} is folded and inactive, due to inhibitory intramolecular interactions (Hiroaki *et al.*, 2001; Groemping *et al.*, 2003; Durand *et al.*, 2006). p40^{phox} is also folded and inactive due to inhibitory intramolecular head-to-tail (PX–PB1) interactions. In the early stages of activation of Nox2, the ternary complex translocates to the phagosome after conformational changes of p47^{phox} that render the PX domain and SH3 domains of p47^{phox} accessible to phospholipids [PI(3,4)P_2, and PA; produced during this stage] and the PR motif of p22^{phox}, respectively. In later stages of activation of Nox2, the ternary complex is retained on the phagosome or may exchange with a cytoplasmic pool after conformational changes in p40^{phox} that render the PX domain of p40^{phox} accessible to bind PI(3)P. In both stages, PKC may stay on the phagosome and phosphorylate p47^{phox}, whereas AA may be a key modulator of conformational changes in p40^{phox} and p47^{phox}. Rac independently translocates to the phagosome.

after phagosome sealing, the carrier or adaptor function of p47^{phox} is replaced by p40^{phox}, whereby the ternary complex interacts with sealed phagosome through PI(3)P specific-binding of the PX domain of p40^{phox}. In this series of interactions, both PKC and AA derived from PLA_2 likely orchestrate conformational changes in p40^{phox} and p47^{phox} that promote their assembly with Nox2 complexes. This model is consistent with recent studies showing that p40^{phox} contributes significantly to phagosomal superoxide production in mouse neutrophils or in FcγIIA receptor and phox-reconstituted COS-7 cells (Ellson *et al*., 2006; Suh *et al*., 2006) and that this requires interactions with the PX, SH3, and PB1 domains of p40^{phox} (Suh *et al*., 2006).

Several lines of evidence suggest AA has important roles in activation of the Nox2 system, although the mechanism of its action is still debated. Many reports emphasize the effects of AA on p47^{phox}. Early studies showed AA or other anionic amphiphiles activate ROS production in cell-free assays of Nox2 activity (Bromberg and Pick, 1984; Curnutte, 1985). It is thought that AA induces conformational changes in p47^{phox} that may mimic the effects of phosphorylation, resulting in exposure of its binding PX and SH3 domains and translocation of p47^{phox} and p67^{phox} (Shiose and Sumimoto, 2000). It was reported that PLA_2 is required for translocation of phox proteins without their phosphorylation (Uhlinger *et al*., 1993; Zhao *et al*., 2002). Others suggested both AA produced by PLA_2- and PKC-dependent phosphorylation together promote translocation of p47^{phox} and enhance ROS production by Nox2 (Sellmayer *et al*., 1996; Shiose and Sumimoto, 2000; Peng *et al*., 2003). We confirmed AA can trigger membrane translocation of p47^{phox}, through interactions involving its PX domain and SH3 domain and that this enables cotranslocation of p67^{phox} (Figures 4 and 6). Other reports suggest exogenous AA has indirect effects on Nox2 activation through downstream AA-derived mediators (Liu *et al*., 2003; Kerkhoff *et al*., 2005; Kim and Dinauer, 2006). Direct involvement of $cPLA_2$ in human Nox2 activation (neutrophils, PLB-985 cells, or monocytes) has been demonstrated using inhibitors or antisense molecules targeted to $cPLA_2$ (Dana *et al*., 1994; Li and Cathcart, 1997; Dana *et al*., 1998; Zhao *et al*., 2002). However, macrophages or neutrophils from $cPLA_2$-deficient mice exhibited normal stimulated ROS release (Gijon *et al*., 2000; Rubin *et al*., 2005), suggesting the murine systems are less dependent on AA. Surprisingly, human $cPLA_2$-deficient cells show normal translocation of phox proteins (Dana *et al*., 1994; Dana *et al*., 1998; Shmelzer *et al*., 2003), suggesting $cPLA_2$ serves other roles in oxidase activation during Nox2 assembly. Interestingly, both $cPLA_2$ and secretory PLA_2 accumulate on newly formed phagosomes (Shmelzer *et al*., 2003; Girotti *et al*., 2004; Balestrieri *et al*., 2006). Furthermore, cells lacking Nox2 show no translocation of $cPLA_2$ to membranes, and it seems that human $cPLA_2$ associates directly with the cytoplasmic phox proteins and the membrane-bound Nox2 complex after stimulation by several agonists that activate the oxidase (Shmelzer *et al*., 2003).

We have now shown that AA triggers the movement of p40^{phox} to PI(3)P-enriched membranes independently of other cytoplasmic phox proteins and that this can enable cotranslocation of p67^{phox}. Although high concentrations of AA (200 μM) were used to observe this phenomenon, 50–100 μM AA also induced translocation (data not shown). Based on our experience, high concentrations of agonists (including AA) are usually required to visualize translocation of GFP-tagged molecules (Shirai *et al*., 1998). It is difficult to estimate the concentrations of AA achieved in whole cells, although high local concentrations of AA may be reached on phagosomes when PLA_2 is recruited during phagocytosis. AA-dependent translocation of p40^{phox} to early endosomes occurs with either N- or C-terminally GFP-tagged p40^{phox}, suggesting the fusions do not influence this process. We propose that this translocation involves AA-induced conformational changes in p40^{phox} that disrupt intramolecular interactions and expose its PX domain to bind membrane lipids, as was suggested in p47^{phox} (Shiose and Sumimoto, 2000). However, in this case we mapped the intramolecular contacts of the p40^{phox} PX domain to its C-terminal PB1 domain.

It is known that p40^{phox} and p67^{phox} associate through homotypic interactions between their PB1 domains (Ito *et al*., 2001; Kuribayashi *et al*., 2002; Wilson *et al*., 2003). The region of p40^{phox} involved was reported as the PC motif (residues 287-302) (Nakamura *et al*., 1998; Ito *et al*., 2001), now referred as the OPR-PC-AID (OPCA) motif (Ponting *et al*., 2002). Later, Wilson *et al*. (2003) showed that Thr337 and Pro339 in the region C-terminal region also participate in the heterodimerization. The importance of this interaction with p67^{phox} was demonstrated with the p40^{phox}(D289A) mutant, which, unlike wild-type p40^{phox}, is unable to stimulate Nox2 activity in PMA or muscarinic receptor-stimulated cells (Kuribayashi *et al*., 2002). This mutation not only interferes with p40^{phox} membrane translocation but also leads to decreased p67^{phox} and p47^{phox} translocation stimulated by PMA. In contrast, in our AA-stimulated model, wild-type or mutant (D289A) GFP-p40^{phox} translocates to early endosomes, even in the absence of p67^{phox} (Figure 3; data not shown). However, we show that a mutation of the PB1 domain in p67^{phox}(K355A) inhibits its cotranslocation with p40^{phox} in AA-stimulated cells (Figure 5). This is the first report proposing an autoinhibitory intramolecular interaction within p40^{phox} between its PX domain and its PB1 domain, because deleting residues 318-328 or replacing this sequence with alanine residues resulted in localization of GFP-p40^{phox} on early endosomes without AA stimulation (Figure 9). Furthermore, we observed the interaction between $(His)_6$-p40^{phox}(PX) and the GST-p40^{phox}(PB1:237-339) (Figure 10B). Crystallographic studies indicate that residues 318-328, encompassing the β-5 strand, do not participate in heterodimerization of p40^{phox} and p67^{phox} (Wilson *et al*., 2003). However, we could not determine which part of the PB1 domain participates in the PX–PB1 interaction of p40^{phox}, because β-5 is part of a β-sheet core structure and deletion or changes of residues 318-328 to alanines could affect the global folding of the PB1 domain of p40^{phox}. It is interesting that sites of phosphorylation in p40^{phox} (Thr154 and Ser315) lie close to the PX domain and residues 318-328 (Bouin *et al*., 1998). Phosphorylation of Thr154, but not Ser315, was proposed as a negative regulator of ROS production by Nox2 (Lopes *et al*., 2004). However, we could not observed significant differences in the subcellular localization between GFP-p40^{phox} and its phosphorylation site mutants [GFP-p40^{phox}(T154A), GFP-p40^{phox}(T154D), GFP-p40^{phox}(S315A), or GFP-p40^{phox}(S315D)], suggesting phosphorylation does not disrupt intramolecular interactions within GFP-p40^{phox}, as seen with AA stimulation. Further studies are needed to clarify whether phosphorylation of p40^{phox} can affect interactions with its PX or PB1 domain or the dynamics of its assembly with the oxidase on phagosomes.

ACKNOWLEDGMENTS

This work was supported in part by a grant-in-aid for scientific research from the 21st Century Center of Excellence Program of the Ministry of Education,

Culture, Sports, Science and Technology of Japan; by a grant-in-aid for scientific research from the Young Scientist of the Ministry of Education, Culture, Sports, Science and Technology in Japan; and by the Uehara Memorial Foundation of Life Science.

REFERENCES

Abo, A., Pick, E., Hall, A., Totty, N., Teahan, C. G., and Segal, A. W. (1991). Activation of the NADPH oxidase involves the small GTP-binding protein p21rac1. Nature *353*, 668–670.

Ago, T., Kuribayashi, F., Hiroaki, H., Takeya, R., Ito, T., Kohda, D., and Sumimoto, H. (2003). Phosphorylation of $p47^{phox}$ directs phox homology domain from SH3 domain toward phosphoinositides, leading to phagocyte NADPH oxidase activation. Proc. Natl. Acad. Sci. USA *100*, 4474–4479.

Ago, T., Takeya, R., Hiroaki, H., Kuribayashi, F., Ito, T., Kohda, D., and Sumimoto, H. (2001). The PX domain as a novel phosphoinositide-binding module. Biochem. Biophys. Res. Commun. *287*, 733–738.

Allen, L. A., DeLeo, F. R., Gallois, A., Toyoshima, S., Suzuki, K., and Nauseef, W. M. (1999). Transient association of the nicotinamide adenine dinucleotide phosphate oxidase subunits $p47^{phox}$ and $p67^{phox}$ with phagosomes in neutrophils from patients with X-linked chronic granulomatous disease. Blood *93*, 3521–3530.

Alloul, N., Gorzalczany, Y., Itan, M., Sigal, N., and Pick, E. (2001). Activation of the superoxide-generating NADPH oxidase by chimeric proteins consisting of segments of the cytosolic component $p67^{phox}$ and the small GTPase Rac1. Biochemistry *40*, 14557–14566.

Ambruso, D. R., *et al*. (2000). Human neutrophil immunodeficiency syndrome is associated with an inhibitory Rac2 mutation. Proc. Natl. Acad. Sci. USA *97*, 4654–4659.

Balestrieri, B., Hsu, V. W., Gilbert, H., Leslie, C. C., Han, W. K., Bonventre, J. V., and Arm, J. P. (2006). Group V secretory phospholipase A_2 translocates to the phagosome after zymosan stimulation of mouse peritoneal macrophages and regulates phagocytosis. J. Biol. Chem. *281*, 6691–6698.

Bokoch, G. M., Bohl, B. P., and Chuang, T. H. (1994). Guanine nucleotide exchange regulates membrane translocation of Rac/Rho GTP-binding proteins. J. Biol. Chem. *269*, 31674–31679.

Bokoch, G. M., and Diebold, B. A. (2002). Current molecular models for NADPH oxidase regulation by Rac GTPase. Blood *100*, 2692–2695.

Bolscher, B. G., van Zwieten, R., Kramer, I. M., Weening, R. S., Verhoeven, A. J., and Roos, D. (1989). A phosphoprotein of Mr 47,000, defective in autosomal chronic granulomatous disease, copurifies with one of two soluble components required for NADPH:O_2 oxidoreductase activity in human neutrophils. J. Clin. Investig. *83*, 757–763.

Bouin, A. P., Grandvaux, N., Vignais, P. V., and Fuchs, A. (1998). $p40^{phox}$ is phosphorylated on threonine 154 and serine 315 during activation of the phagocyte NADPH oxidase. J. Biol. Chem. *273*, 30097–30103.

Bravo, J., *et al*. (2001). The crystal structure of the PX domain from $p40^{phox}$ bound to phosphatidylinositol 3-phosphate. Mol. Cell. *8*, 829–839.

Bromberg, Y., and Pick, E. (1984). Unsaturated fatty acids stimulate NADPH-dependent superoxide production by cell-free system derived from macrophages. Cell Immunol. *88*, 213–221.

Brown, G. E., Stewart, M. Q., Liu, H., Ha, V. L., and Yaffe, M. B. (2003). A novel assay system implicates PtdIns(3,4)P_2, PtdIns(3)P, and PKCδ in intracellular production of reactive oxygen species by the NADPH oxidase. Mol. Cell *11*, 35–47.

Cross, A. R. (2000). $p40^{phox}$ participates in the activation of NADPH oxidase by increasing the affinity of $p47^{phox}$ for flavocytochrome b_{558}. Biochem. J. *349*, 113–117.

Curnutte, J. T. (1985). Activation of human neutrophil nicotinamide adenine dinucleotide phosphate, reduced (triphosphopyridine nucleotide, reduced) oxidase by arachidonic acid in a cell-free system. J. Clin. Investig. *75*, 1740–1743.

Dana, R., Leto, T. L., Malech, H. L., and Levy, R. (1998). Essential requirement of cytosolic phospholipase A_2 for activation of the phagocyte NADPH oxidase. J. Biol. Chem. *273*, 441–445.

Dana, R., Malech, H. L., and Levy, R. (1994). The requirement for phospholipase A_2 for activation of the assembled NADPH oxidase in human neutrophils. Biochem. J. *297*, 217–223.

de Mendez, I., Garrett, M. C., Adams, A. G., and Leto, T. L. (1994). Role of p67-phox SH3 domains in assembly of the NADPH oxidase system. J. Biol. Chem. *269*, 16326–16332.

de Mendez, I., Homayounpour, N., and Leto, T. L. (1997). Specificity of $p47^{phox}$ SH3 domain interactions in NADPH oxidase assembly and activation. Mol. Cell. Biol. *17*, 2177–2185.

Duclos, S., Diez, R., Garin, J., Papadopoulou, B., Descoteaux, A., Stenmark, H., and Desjardins, M. (2000). Rab5 regulates the kiss and run fusion between phagosomes and endosomes and the acquisition of phagosome leishmanicidal properties in RAW 264.7 macrophages. J. Cell Sci. *113*, 3531–3541.

Durand, D., Cannella, D., Dubosclard, V., Pebay-Peyroula, E., Vachette, P., and Fieschi, F. (2006). Small-angle X-ray scattering reveals an extended organization for the autoinhibitory resting state of the $p47^{phox}$ modular protein. Biochemistry *45*, 7185–7193.

Dusi, S., Donini, M., and Rossi, F. (1996). Mechanisms of NADPH oxidase activation: translocation of $p40^{phox}$, Rac1 and Rac2 from the cytosol to the membranes in human neutrophils lacking $p47^{phox}$ or $p67^{phox}$. Biochem. J. *314*, 409–412.

Ellson, C. D., Anderson, K. E., Morgan, G., Chilvers, E. R., Lipp, P., Stephens, L. R., and Hawkins, P. T. (2001a). Phosphatidylinositol 3-phosphate is generated in phagosomal membranes. Curr. Biol. *11*, 1631–1635.

Ellson, C. D., Davidson, K., Ferguson, G. J., O'Connor, R., Stephens, L. R., and Hawkins, P. T. (2006). Neutrophils from $p40^{phox-/-}$ mice exhibit severe defects in NADPH oxidase regulation and oxidant-dependent bacterial killing. J. Exp. Med. *203*, 1927–1937.

Ellson, C. D., *et al*. (2001b). PtdIns(3)P regulates the neutrophil oxidase complex by binding to the PX domain of $p40^{phox}$. Nat. Cell Biol. *3*, 679–682.

Freeman, J. L., and Lambeth, J. D. (1996). NADPH Oxidase Activity Is Independent of $p47^{phox}$ in Vitro. J. Biol. Chem. *271*, 22578–22582.

Gijon, M. A., Spencer, D. M., Siddiqi, A. R., Bonventre, J. V., and Leslie, C. C. (2000). Cytosolic phospholipase A_2 is required for macrophage arachidonic acid release by agonists that Do and Do not mobilize calcium. J. Biol. Chem. *275*, 20146–20156.

Gillooly, D. J., Morrow, I. C., Lindsay, M., Gould, R., Bryant, N. J., Gaullier, J. M., Parton, R. G., and Stenmark, H. (2000). Localization of phosphatidylinositol 3-phosphate in yeast and mammalian cells. EMBO J. *19*, 4577–4588.

Gillooly, D. J., Simonsen, A., and Stenmark, H. (2001). Phosphoinositides and phagocytosis. J. Cell Biol. *155*, 15–17.

Girotti, M., Evans, J. H., Burke, D., and Leslie, C. C. (2004). Cytosolic Phospholipase A_2 Translocates to Forming Phagosomes during Phagocytosis of Zymosan in Macrophages. J. Biol. Chem. *279*, 19113–19121.

Gorzalczany, Y., Sigal, N., Itan, M., Lotan, O., and Pick, E. (2000). Targeting of Rac1 to the phagocyte membrane is sufficient for the induction of NADPH oxidase assembly. J. Biol. Chem. *275*, 40073–40081.

Grizot, S., *et al*. (2001). Small angle neutron scattering and gel filtration analyses of neutrophil NADPH oxidase cytosolic factors highlight the role of the C-terminal end of $p47^{phox}$ in the association with $p40^{phox}$. Biochemistry *40*, 3127–3133.

Groemping, Y., Lapouge, K., Smerdon, S. J., and Rittinger, K. (2003). Molecular basis of phosphorylation-induced activation of the NADPH oxidase. Cell *113*, 343–355.

Gu, Y., *et al*. (2003). Hematopoietic cell regulation by Rac1 and Rac2 guanosine triphosphatases. Science *302*, 445–449.

Han, C. H., Freeman, J. L., Lee, T., Motalebi, S. A., and Lambeth, J. D. (1998). Regulation of the neutrophil respiratory burst oxidase. Identification of an activation domain in $p67^{phox}$. J. Biol. Chem. *273*, 16663–16668.

He, R., Nanamori, M., Sang, H., Yin, H., Dinauer, M. C., and Ye, R. D. (2004). Reconstitution of chemotactic peptide-induced nicotinamide adenine dinucleotide phosphate (reduced) oxidase activation in transgenic COS-phox cells. J. Immunol. *173*, 7462–7470.

Heyworth, P., Bohl, B., Bokoch, G., and Curnutte, J. (1994). Rac translocates independently of the neutrophil NADPH oxidase components $p47^{phox}$ and $p67^{phox}$. Evidence for its interaction with flavocytochrome b_{558}. J. Biol. Chem. *269*, 30749–30752.

Heyworth, P. G., Curnutte, J. T., Nauseef, W. M., Volpp, B. D., Pearson, D. W., Rosen, H., and Clark, R. A. (1991). Neutrophil nicotinamide adenine dinucleotide phosphate oxidase assembly. J. Clin. Investig. *87*, 352–356.

Hiroaki, H., Ago, T., Ito, T., Sumimoto, H., and Kohda, D. (2001). Solution structure of the PX domain, a target of the SH3 domain. Nat. Struct. Biol. *8*, 526–530.

Ito, T., Matsui, Y., Ago, T., Ota, K., and Sumimoto, H. (2001). Novel modular domain PB1 recognizes PC motif to mediate functional protein-protein interactions. EMBO J. *20*, 3938–3946.

Jesaitis, A. J., Buescher, E. S., Harrison, D., Quinn, M. T., Parkos, C. A., Livesey, S., and Linner, J. (1990). Ultrastructural localization of cytochrome *b*

in the membranes of resting and phagocytosing human granulocytes. J. Clin. Investig. *85*, 821–835.

Kami, K., Takeya, R., Sumimoto, H., and Kohda, D. (2002). Diverse recognition of non-PxxP peptide ligands by the SH3 domains from p67^{phox}, Grb2 and Pex13p. EMBO. J. *21*, 4268–4276.

Kanai, F., Liu, H., Field, S. J., Akbary, H., Matsuo, T., Brown, G. E., Cantley, L. C., and Yaffe, M. B. (2001). The PX domains of p47^{phox} and p40^{phox} bind to lipid products of PI(3)K. Nat. Cell Biol. *3*, 675–678.

Karathanassis, D., Stahelin, R. V., Bravo, J., Perisic, O., Pacold, C. M., Cho, W., and Williams, R. L. (2002). Binding of the PX domain of p47^{phox} to phosphatidylinositol 3,4-bisphosphate and phosphatidic acid is masked by an intramolecular interaction. EMBO J. *21*, 5057–5068.

Kerkhoff, C., Nacken, W., Benedyk, M., Dagher, M. C., Sopalla, C., and Doussiere, J. (2005). The arachidonic acid-binding protein S100A8/A9 promotes NADPH oxidase activation by interaction with p67^{phox} and Rac-2. FASEB J. *19*, 467–469.

Kim, C., and Dinauer, M. C. (2006). Impaired NADPH oxidase activity in Rac2-deficient murine neutrophils does not result from defective translocation of p47^{phox} and p67^{phox} and can be rescued by exogenous arachidonic acid. J. Leukoc. Biol. *79*, 223–234.

Knaus, U. G., Heyworth, P. G., Evans, T., Curnutte, J. T., and Bokoch, G. M. (1991). Regulation of phagocyte oxygen radical production by the GTP-binding protein Rac 2. Science *254*, 1512–1515.

Koshkin, V., Lotan, O., and Pick, E. (1996). The cytosolic component p47^{phox} is not a sine qua non participant in the activation of NADPH oxidase but is required for optimal superoxide production. J. Biol. Chem. *271*, 30326–30329.

Kuribayashi, F., Nunoi, H., Wakamatsu, K., Tsunawaki, S., Sato, K., Ito, T., and Sumimoto, H. (2002). The adaptor protein p40^{phox} as a positive regulator of the superoxide-producing phagocyte oxidase. EMBO J. *21*, 6312–6320.

Lapouge, K., Smith, S. J., Groemping, Y., and Rittinger, K. (2002). Architecture of the p40-p47-p67^{phox} complex in the resting state of the NADPH oxidase. J. Biol. Chem. *277*, 10121–10128.

Larsen, E. C., Ueyama, T., Brannock, P. M., Shirai, Y., Saito, N., Larsson, C., Loegering, D., Weber, P. B., and Lennartz, M. R. (2002). A role for PKC-ε in FcγR-mediated phagocytosis by RAW 264.7 cells. J. Cell Biol. *159*, 939–944.

Leto, T., Garrett, M., Fujii, H., and Nunoi, H. (1991). Characterization of neutrophil NADPH oxidase factors p47^{phox} and p67^{phox} from recombinant baculoviruses. J. Biol. Chem. *266*, 19812–19818.

Leto, T. L. (1999). The respiratory burst oxidase. In: Inflammation: Basic Principles and Clinical Correlates, ed. J. I. Gallin and R. Snyderman, Philadelphia: Lippincott Williams & Wilkins, 769–787.

Leto, T. L., Adams, A. G., and de Mendez, I. (1994). Assembly of the phagocyte NADPH oxidase: binding of Src homology 3 domains to proline-rich targets. Proc. Natl. Acad. Sci. USA *91*, 10650–10654.

Li, Q., and Cathcart, M. K. (1997). Selective inhibition of cytosolic phospholipase A_2 in activated human monocytes. Regulation of superoxide anion production and low density lipoprotein oxidation. J. Biol. Chem. *272*, 2404–2411.

Liu, J., Liu, Z., Chuai, S., and Shen, X. (2003). Phospholipase C and phosphatidylinositol 3-kinase signaling are involved in the exogenous arachidonic acid-stimulated respiratory burst in human neutrophils. J. Leukoc. Biol. *74*, 428–437.

Lopes, L. R., Dagher, M. C., Gutierrez, A., Young, B., Bouin, A. P., Fuchs, A., and Babior, B. M. (2004). Phosphorylated p40^{phox} as a negative regulator of NADPH oxidase. Biochemistry *43*, 3723–3730.

Massenet, C., Chenavas, S., Cohen-Addad, C., Dagher, M.-C., Brandolin, G., Pebay-Peyroula, E., and Fieschi, F. (2005). Effects of p47^{phox} C Terminus Phosphorylations on Binding Interactions with p40^{phox} and p67^{phox}. J. Biol. Chem. *280*, 13752–13761.

Nakamura, R., Sumimoto, H., Mizuki, K., Hata, K., Ago, T., Kitajima, S., Takeshige, K., Sakaki, Y., and Ito, T. (1998). The PC motif: a novel and evolutionarily conserved sequence involved in interaction between p40^{phox} and p67^{phox}, SH3 domain-containing cytosolic factors of the phagocyte NADPH oxidase. Eur. J. Biochem. *251*, 583–589.

Nauseef, W. M. (2004). Assembly of the phagocyte NADPH oxidase. Histochem. Cell Biol. *122*, 277–291.

Peng, G., Huang, J., Boyd, M., and Kleinberg, M. E. (2003). Properties of phagocyte NADPH oxidase p47-phox mutants with unmasked SH3 (Src homology 3) domains: full reconstitution of oxidase activity in a semi-recombinant cell-free system lacking arachidonic acid. Biochem. J. *373*, 221–229.

Ponting, C. P., Ito, T., Moscat, J., Diaz-Meco, M. T., Inagaki, F., and Sumimoto, H. (2002). OPR, PC and AID: all in the PB1 family. Trends Biochem. Sci. *27*, 10.

Quinn, M. T., and Gauss, K. A. (2004). Structure and regulation of the neutrophil respiratory burst oxidase: comparison with nonphagocyte oxidases. J. Leukoc. Biol. *76*, 760–781.

Roberts, A. W., *et al*. (1999). Deficiency of the hematopoietic cell-specific Rho family GTPase Rac2 is characterized by abnormalities in neutrophil function and host defense. Immunity *10*, 183–196.

Rotrosen, D., and Leto, T. L. (1990). Phosphorylation of neutrophil 47-kDa cytosolic oxidase factor. J. Biol. Chem. *265*, 19910–19915.

Rubin, B. B., *et al*. (2005). Cytosolic phospholipase A_2-α is necessary for platelet-activating factor biosynthesis, efficient neutrophil-mediated bacterial killing, and the innate immune response to pulmonary infection. J. Biol. Chem. *280*, 7519–7529.

Sathyamoorthy, M., de Mendez, I., Adams, A. G., and Leto, T. L. (1997). p40(phox) down-regulates NADPH oxidase activity through interactions with its SH3 domain. J. Biol. Chem. *272*, 9141–9146.

Sellmayer, A., Obermeier, H., Danesch, U., Aepfelbacher, M., and Weber, P. C. (1996). Arachidonic acid increases activation of NADPH oxidase in monocytic U937 cells by accelerated translocation of p47-phox and co-stimulation of protein kinase C. Cell Signal *8*, 397–402.

Shiose, A., and Sumimoto, H. (2000). Arachidonic acid and phosphorylation synergistically induce a conformational change of p47^{phox} to activate the phagocyte NADPH oxidase. J. Biol. Chem. *275*, 13793–13801.

Shirai, Y., Kashiwagi, K., Yagi, K., Sakai, N., and Saito, N. (1998). Distinct effects of fatty acids on translocation of γ- and ε-subspecies of protein kinase C. J. Cell Biol. *143*, 511–521.

Shmelzer, Z., Haddad, N., Admon, E., Pessach, I., Leto, T. L., Eitan-Hazan, Z., Hershfinkel, M., and Levy, R. (2003). Unique targeting of cytosolic phospholipase A_2 to plasma membranes mediated by the NADPH oxidase in phagocytes. J. Cell Biol. *162*, 683–692.

Suh, C.-I., Stull, N. D., Li, X. J., Tian, W., Price, M. O., Grinstein, S., Yaffe, M. B., Atkinson, S., and Dinauer, M. C. (2006). The phosphoinositide-binding protein p40^{phox} activates the NADPH oxidase during FcγIIA receptor-induced phagocytosis. J. Exp. Med. *203*, 1915–1925.

Sumimoto, H., Hata, K., Mizuki, K., Ito, T., Kage, Y., Sakaki, Y., Fukumaki, Y., Nakamura, M., and Takeshige, K. (1996). Assembly and activation of the phagocyte NADPH oxidase. J. Biol. Chem. *271*, 22152–22158.

Sumimoto, H., Kage, Y., Nunoi, H., Sasaki, H., Nose, T., Fukumaki, Y., Ohno, M., Minakami, S., and Takeshige, K. (1994). Role of Src homology 3 domains in assembly and activation of the phagocyte NADPH oxidase. Proc. Natl. Acad. Sci. USA *91*, 5345–5349.

Tsunawaki, S., Kagara, S., Yoshikawa, K., Yoshida, L. S., Kuratsuji, T., and Namiki, H. (1996). Involvement of p40^{phox} in activation of phagocyte NADPH oxidase through association of its carboxyl-terminal, but not its amino-terminal, with p67^{phox}. J. Exp. Med. *184*, 893–902.

Ueyama, T., Eto, M., Kami, K., Tatsuno, T., Kobayashi, T., Shirai, Y., Lennartz, M. R., Takeya, R., Sumimoto, H., and Saito, N. (2005). Isoform-specific membrane targeting mechanism of Rac during FcγR-mediated phagocytosis: positive charge-dependent and independent targeting mechanism of Rac to the phagosome. J. Immunol. *175*, 2381–2390.

Ueyama, T., *et al*. (2004). Superoxide production at phagosomal cup/phagosome through βI protein kinase C during FcγR-mediated phagocytosis in microglia. J. Immunol. *173*, 4582–4589.

Ueyama, T., Ren, Y., Sakai, N., Takahashi, M., Ono, Y., Kondoh, T., Tamaki, N., and Saito, N. (2001). Generation of a constitutively active fragment of PKN in microglia/macrophages after middle cerebral artery occlusion in rats. J. Neurochem. *79*, 903–913.

Uhlinger, D. J., Tyagi, S. R., Inge, K. L., and Lambeth, J. D. (1993). The respiratory burst oxidase of human neutrophils. Guanine nucleotides and arachidonate regulate the assembly of a multicomponent complex in a semi-recombinant cell-free system. J. Biol. Chem. *268*, 8624–8631.

van Bruggen, R., Anthony, E., Fernandez-Borja, M., and Roos, D. (2004). Continuous translocation of Rac2 and the NADPH oxidase component p67^{phox} during phagocytosis. J. Biol. Chem. *279*, 9097–9102.

Vergnaud, S., Paclet, M. H., El Benna, J., Pocidalo, M. A., and Morel, F. (2000). Complementation of NADPH oxidase in p67^{phox}-deficient CGD patients p67^{phox}/p40^{phox} interaction. Eur. J. Biochem. *267*, 1059–1067.

Williams, D. A., *et al*. (2000). Dominant negative mutation of the hematopoietic-specific Rho GTPase, Rac2, is associated with a human phagocyte immunodeficiency. Blood *96*, 1646–1654.

Wilson, M. I., Gill, D. J., Perisic, O., Quinn, M. T., and Williams, R. L. (2003). PB1 domain-mediated heterodimerization in NADPH oxidase and signaling complexes of atypical protein kinase C with Par6 and p62. Mol. Cell *12*, 39–50.

Zhao, T., Benard, V., Bohl, B. P., and Bokoch, G. M. (2003). The molecular basis for adhesion-mediated suppression of reactive oxygen species generation by human neutrophils. J. Clin. Investig. *112*, 1732–1740.

Zhao, X., Bey, E. A., Wientjes, F. B., and Cathcart, M. K. (2002). Cytosolic phospholipase A_2 ($cPLA_2$) regulation of human monocyte NADPH oxidase activity. $cPLA_2$ affects translocation but not phosphorylation of $p67^{phox}$ and $p47^{phox}$. J. Biol. Chem. *277*, 25385–25392.